DESIGN AND SIMULATION OF A CONTROL SYSTEM FOR A HYBRID LIFT ASSIST DEVICE

by

Dhaval D. Patel

A thesis submitted to the faculty of
The University of Utah
in partial fulfillment of the requirements for the degree of

Master of Science

Department of Mechanical Engineering

The University of Utah

December 2012

The University of Utah Graduate School

STATEMENT OF THESIS APPROVAL

The thesis of **Dhaval D. Patel** has been approved by the following supervisory committee members:

Andrew S. Merryweather , Chair	**01/04/2012** Date of Approval
Donald S. Bloswick , Member	**01/04/2012** Date of Approval
Stacy J. M. Bamberg , Member	**01/04/2012** Date of Approval

and by **Timothy A. Ameel** , Chair of the Department of **Mechanical Engineering** and by Charles A. Wight, Dean of the Graduate School.

ABSTRACT

Manual Material Handing (MMH) is a common activity for many workers in the workplace. Back compressive force has been described as a leading factor causing back injuries and musculoskeletal disorders (MSD) associated with lifting. To prevent such injuries, mechanical Lift Assist Devices (LAD) have been developed. To improve device usability and allow more interaction with human body movements, a significant step has been taken towards developing an automatic feedback control system for a hybrid lift assist device. The control system is highly responsive which would likely result in a reduction of required erector spine muscle force during lifting tasks. The control system is based on multiple input and multiple output (MIMO).This design was chosen to control the outputs of Torque (τ) and Speed (ω) generated from a DC motor from the inputs: hip angle, torso angle and HD (Horizontal Distance from L5/S1 to center of load derived from the Force and Center of Pressure (COP) using Flexi Force Sensors in the shoe insole). All the inputs were derived and compared with parameters of human body movement recorded using Vicon Nexus and 8 Bonita cameras. The Utah Back Compressive model was used to estimate the desired torque required by the LAD. The motor is controlled to generate the amount of torque to lift the load and to assist the body to a specified percent assist (0-100%). The design of the control system was achieved using a proper controller and DC motor with a closed loop feedback system. The control

system produces reliable and robust performance for a variety of sagittal plane lifting techniques. This was accomplished by deriving the system input parameters from measurable device features and fine tuning the controller and selected DC motor model. These results indicate that a hybrid lifting assist device is feasible and can be programmed to provide variable assistance during lifting tasks.

TABLE OF CONTENTS

LIST OF FIGURES

Figure

LIST OF TABLES

Table

ACKNOWLEDGEMENTS

Firstly, I would like to express my deepest gratitude to my advisor Dr. Andrew S. Merryweather for his excellent guidance, constant support and encouragement to accomplish my research project. I am very grateful to Dr. Don Bloswick and Dr. Stacy Bamberg for being part of my committee, and I am honored for their valuable suggestions.

I would also like to thank my parents, elder sisters, and brother in-law. They were always supporting me and encouraging me with their best wishes.

Last but not least, I would like to thank all my colleges and especially students of Ergonomics & Safety Lab for their great support and help.

1. INTRODUCTION

Lift Assist Devices (LAD) were developed in an effort to reduce lower back injuries from lifting loads. Low back pain is among the most common musculoskeletal complaints from people working in the industrialized world as they account for 25% of workers' compensation claims in the US[1]. The total cost of low back pain disorders in the United States has been estimated to be approximately $72 billion [2] and it is steadily increasing[3]. One solution to reducing worker exposure to forceful exertions while lifting is to automate material handling processor provides equipment designed to handle objects. Often, if given the opportunity, workers will choose not to use these assist devices because they add more time for the operation than manually handling the load, or the devices create new undesirable and awkward force requirements, such as initiating movement and working against momentum to stop and position the load. Or they prefer to use manually operated devices. Keeping those factors in mind, more flexible and portable devices have been developed, as shown in Figure 1, Torsion spring LAD, Bending LAD and Commercial Assisting Device "Springzback™"[4]. These devices are flexible and more practical to use and help workers to prevent from back injuries and musculoskeletal disorders. Additional, simple devices like PLAD have been developed and tested and continue to show positive results [5], [6].

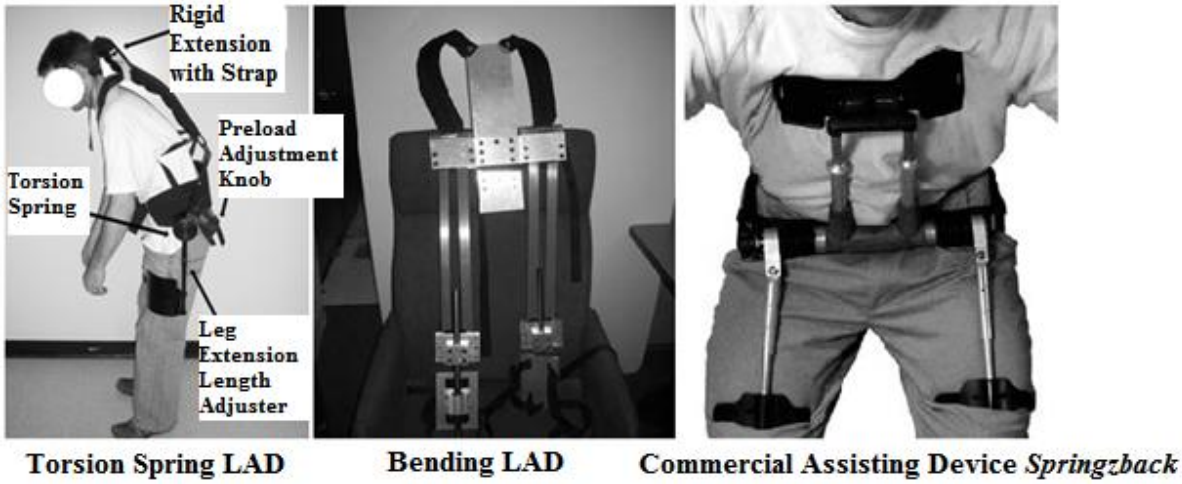

Figure 1 Developed Lift Assist Devices

2. BACKGROUND

2.1 Back Injury

Back injuries are a subset of musculoskeletal disorder (MSD)[7]. Back injury results from damage, wear or trauma to the bones, vertebral disks and muscles of the back. Back injuries are the most common cause of back pain. Common back injuries include sprains and strains, bulging discs and fractured vertebrae. The lumbar region is often the site of back pain. The nerves that provide sensation and stimulate the muscles of the low back as well as the lower extremities exit the lumbar spinal column through bony portals, each of which is called foramen[8]. Many muscle groups are responsible for flexing, extending, and rotating the torso as well as the lower extremities. These muscles attach to the lumbar spine at tendon insertions sites. Often, low back pain results from frequent lifting or lifting with awkward posture and highly repetitive lifting, bending and twisting motions of the torso which affect both the severity and frequency of low-back pain[9]. While lifting a heavy load, the horizontal distance (HD) of the load to the lumbosacral disc (L5/S1) is the primary factor that influences moment.

In a study conducted by Bureau of Labor Statistics (BLS) on the Injuries and Illness, casesconcentrated more on lower back of the bodywhich determines the number of cases for back injury[10]. Figure 2 shows the change in number of back injuries per year.

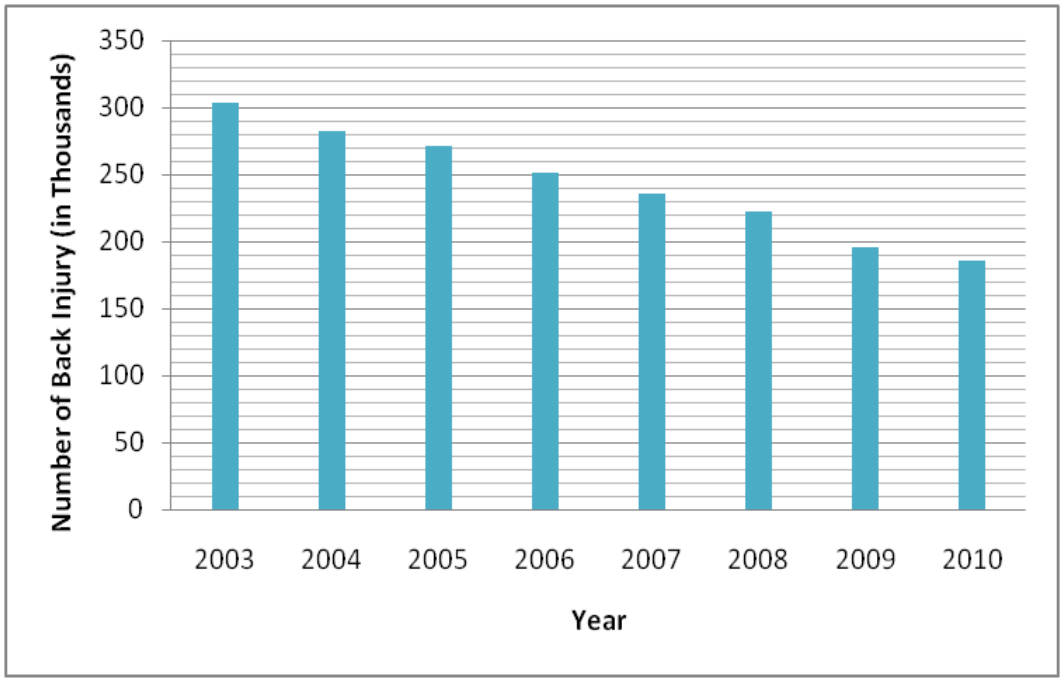

Figure 2 Rate of Back Injury

Here we can see that number of injuries are decreasing year by year, one of the reasonsfor this trend is likely that more and more studies having been done on back injuries and many jobs include full or semi-automated processes. More and more studies contribute to better understanding of casual factors of low back pain and result in workplace improvements. This is one of the major reasons we feel this research and design are important. Lifting assist devices can be directly or indirectly designed to assist workers in industryand prevent back injury. There is also a potential that these devices could be implemented for rehabilitation and out-patient care.

The complex structure of the lower back enables it to tolerate relatively high compressive loads. In most cases, back pain is the result of strain on the soft tissues of the

back, such as muscles, tendons and ligaments[11]. These tissues can be injured if this tolerance is exceeded.

Some work related risk factors are the major reasons for Low Back Pain (LBP):

- Heavy physical work force
- Static work postures
- Frequent bending or twisting
- Lifting, pushing and pulling
- Repetitive work
- Reach of the lifting load

These risk factors have been associated with the development of low back pain. The direct relationship between an adverse outcome (back pain) and each factor is largely unknown; however, the result of exposure to heavy physical work is largely a function of applied force, awkward body posture and, high repetition frequency and duration. Improper technique of lifting, pulling or pushing might increase the stress on the back muscles which can lead to muscle fatigue and Upper Extremity Musculoskeletal Disorders (UEMSD)[12].

In Back Injury, it is often difficult to accurately pinpoint which muscles or ligaments have been damaged as a result of an injury. It is important to remember that once injured, the back can become susceptible to re-injury, especially if there are risk factors in the workplace that are not corrected. Risk factors are aspects of a task that are associated with an increased risk of developing an injury. The risk increases further if there is a combination of two or more risk factors found in the same task.

2.2 Back Rehabilitation

Rehabilitation is the process that helps patients to recover from an injury or surgery as quickly as possible. Rehabilitation exercise and physical therapy are two forms of back rehabilitation. Initially for a treatment, physical therapists work on the patient to get them back to an improved state just after the back surgery. Conservative treatments for back injury and pain include basic treatments, exercise, work, restrictions, manipulation therapy and others before recommending surgery[13]. They first try minimally-invasive methods such as injections. That will cost around $2500[14]. If there is no improvement in condition then an operation with endoscopic instruments, which costs $8000, is performed. If the pain continues, then the patient has to undergo Laminectomy surgery, which costs $85,000[14].

One of our research objectives is to develop a type of rehabilitation device that helps a person treat mild cases of back pain problems without surgery. This device is also applicable in industry for lifting heavy loads or high frequency lifting tasks to reduce the compressive forces caused from erector spine muscle activity. If a person reports back pain early, this device can provide assistance to alleviate stress and act to reduce the stress caused by one's own body weight during the task. The major advantage of using this device is low cost with no other side effects on the body. This device may prove to be an inexpensive alternative to surgery and reduces the indirect expenses incurred from other noninvasive conservative treatments for low back pain.

After back surgery, this device may be used as a rehabilitation device to slowly reduce assistance during lifting and help workers reenter a job after an injury.

2.3 Back Compressive Force

Back Compressive Force (BCF) increases during manual material handling (MMH) like pushing or pulling and lifting and lowering[15]. These tasks directly affect L5/S1 joint by compressive forces [15]. BCF is commonly determined by static back compressive force values at the origin and the destination of the lift and lifting speed [16]. In an improved biomechanical model, a dynamic factor provided more accurate results to get the BCF on the spine during lifting [16].Using the dynamic factor and other static conditions, the back compressive force on the L5/S1 can be derived by the following equations[17]:

$$BCF = A + B + C \qquad \text{Equation (1)}$$

$$A = 0.0167 * BW * HT * \sin\theta \qquad \text{Equation (1.1)}$$

$$B = 0.145 * L * HB \qquad \text{Equation (1.2)}$$

$$C = 0.8 * \left[\frac{BW}{2} + L\right] \qquad \text{Equation (1.3)}$$

A = Back muscle force reactive to the upper body weight.

B = Back muscle force reacting to load moment.

C = Direct compressive component of upper body weight and load in hand.

2.4 Assist Devices

Many assist devices (mechanical and automated) have been developed to serve the purpose of providing assistance during lifting or material handling. In this study an

attempt is made to develop a control system for semiautomated LAD to improve passive assist devices and improve the dynamic performance of the system. In another category of assist devices are fully automatic systems called Exoskeletons. One of these devices was developed at the Berkeley Robotics and Human Engineering Laboratory. The project is called Berkeley Lower Extremity Exoskeleton (BLEEX) because it lies under the study of the lower extremity[18].

The existing mechanical assist devices on the market are used as an aid in the prevention and rehabilitation of low back injuries. These devices are mechanically operated by force or torque to provide the assistance to the body while lifting to lower risk of injury or enhance human capabilities. The fully automatic exoskeleton devices that are operated with hydraulic or pneumatic systems to apply the forces for higher amount of work efficiency and accuracy are prohibitive because they limit flexibility and portability. A passive LAD is very easy to access in smaller work areas and the cost is much lower. In Figure 3, the LAD with Torsion spring [4] is unique. This device was developed at the University of Utah. Another study into the effectiveness of LADs to reduce back strain and act as a rehabilitation device after an injury on the back was conducted by Chris Brammer[4].

Torsion Spring device provides the percent of assistance by producing the amount of torque required to support the upper body weight using a torsion spring. The spring is connected to the device near the hip joint, and a torsion knob provides the preload to adjust the percent of assistance supplied. It works as the torso bends the energy is stored in the spring at the same time it supports the upper body by generating a resisting torque which also reduces the BCF (Back Compressive Force) in the spine.

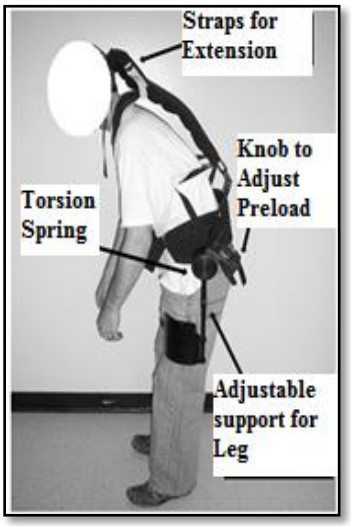

Figure 3 Torsion Spring LAD [4]

Reprinted with Permission

This device is light weight and it has more flexibility to adjust according to the body posture such as adjustable waist support, backpack straps and adjustable webbing straps attached to the backpack straps. Moreover the leg extension, torso extension and device width for both the sides are adjustable in length, which provides proper leg extension and flexion according to the torso movement.

The device shown in Figure 4 is called Bending LAD [4]. It serves the same purpose but in a different way because of the structure. This LAD is made with two fiberglass thin bending members that are used as the straps on the back. While bending the torso, some energy is stored in the fiberglass members. As the body straightens energy gets released from the member in the form of a support moment about the hips. This device is used to provide assistance when the body is flexed. It provides proper support to the back and the legs and adjusts with the leg position.

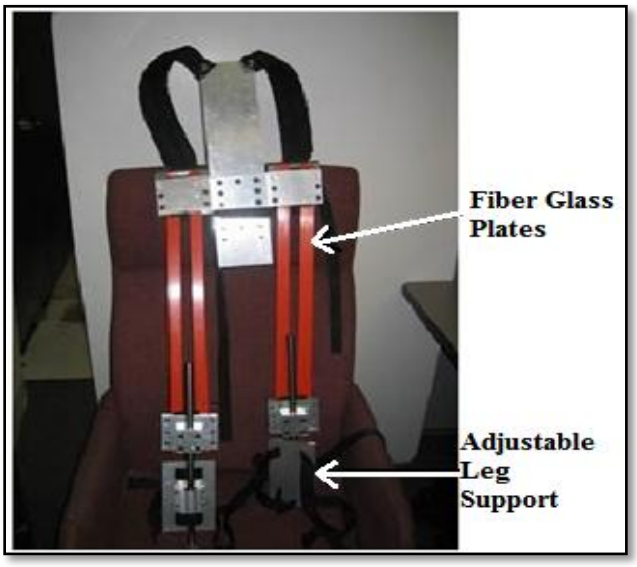

Figure 4 Bending LAD [4]

Reprinted with Permission

There are few drawbacks with this device.It is heavier than the torsion spring LAD and theSpringzback™[18] and it does not have enough cushioning to be comfortable. Besides these drawbacks it has good structure to give better flexibility and proper shape to the body. Improvements could be made, such as using proper material with more cushioning for straps. Use of aluminium or other light weight material for the structure development of the Bending lift assist device to reduce the unwanted extra weight. The device provides another platform to start to analyze the effectiveness of LADs.

The device in Figure 5 is called *Springzback*™[18], which is a commercially available assisting device used as a LAD. This device provides support to the upper body while bending forward, which also eliminates the strain from the lower back muscle.

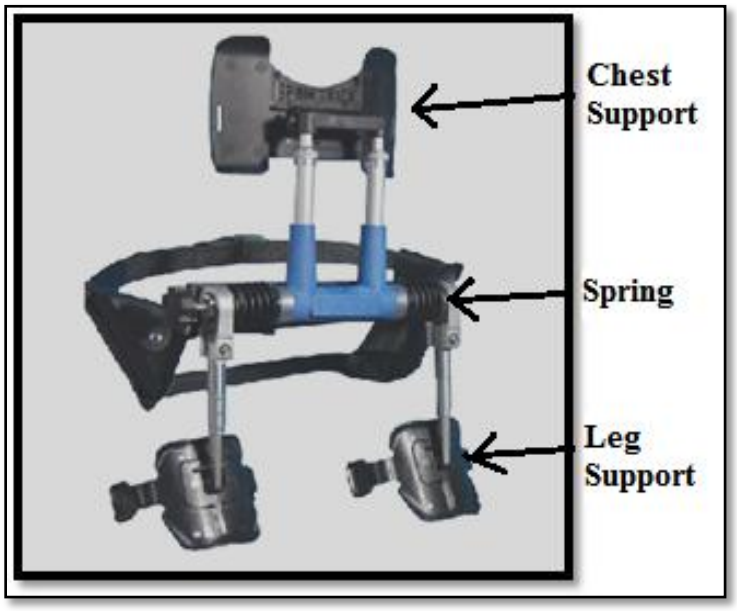

Figure 5 SPRINGZBACK™ Device (Copyright © 2011 Babcock Innovations, Inc) Reprinted with Permission

The Springzback™ device supports the upper body with a lumbar belt, and while bending forward, transfers the weight of the upper body to the legs[18]. This device provides adjustability by varying the amount of assistance with a regulating the knob on the left hand side of the device. This device is padded on the front chest support and is designed to fit on the anterior side of the thighs. It attaches to the user with a specialized belt that is also adjustable and flexible to accommodate different body shapes and sizes.

This device is very portable, compact and lightweight as compared to other devices. The major limitation as noted by Brammer[4] is the ability to actively respond to movement. This device is better suited for static working positions, including standing and kneeling.

All three devices are different from each other in structure and design, but work off the same concept of moment generation around the hips. With the torsion spring and

Springzback™ the assistance rate can be regulated in both devices by adjusting the spring preload.

One more device which has been developed with more advanced technology as mentioned before is the Berkeley Exoskeleton. As shown in Figure 6, this device is very hi-tech and is not applicable for everyday life. The device has a very advanced mechanism where it can provide support the human body. The device has been developed for the purpose of defense rather than work, and has applications for disaster relief workers, wildfire fighters and similar emergency personnel[19].

Figure 6 Exoskeleton by BLEEX (Copyright © Berkeley Lower Extremity Exoskeleton, 2004) Reprinted with Permission

This exoskeleton design is elaborate and should not be directly compared to the system presented in this thesis. The Berkeley Exoskeleton device is not particularly developed for reducing back stress and strain, but rather for enhancing strength to the whole body.

2.5 Scope of this Study

From the background of this study there are many LADs developed in an effort to reduce back compressive forces while lifting. All these devices are either purely mechanical or very hi-tech like the Berkeley Exoskeleton. To acquire the same purpose by providing a reliable combination of mechanical and electronic control system and that can be utilized as a base line to develop a real device such as hybrid lift assist device. There have been many studies done in the past for developing such LADs. But none of them introduced major factors like COP and HD, which are major parameters for developing an automated LAD. Using these parameters it is easy to obtain the travel direction of the load, load location and magnitude of the load.

The main goal behind this study is to develop a control system for a future LAD with properly defined input functions and hardware parameters that can provide optimal performance to the user to perform a variety of lifting tasks with different body postures. This control system incorporates the Dynamic Model studied as a foundation of this system, feedback control system and working of the PID controller. This study also describes the established function for predicted HD using force and COP data from FFS and angle data. Hence the part of this study can be written in terms of hypotheses as:

Hypothesis I: HD values predicted from derived function and HD values calculated directly from the motion capture system are equal.

Hypothesis II: The COP values calculated from FFS and COP values measured from force plate are equal.

Hypothesis III: Force values calculated from FFS and force measured directly from force plate data are equal.

3. METHOD

In this section model development was discussed first, and was used as logic to build and design the control system for the lift assist device. Following a discussion of the model, the control system is described based on the selected controller and controlling method. Finally the data collection methods along with the setup to collect the data are discussed. In this study there were two types of data collected:

1) The force and COP were collected using FFSs and HD, torso and hip angle data were collected using different methods. All these data were used as input parameters of the control system.
2) The force, COP, HD, torso and hip angle data were collected using the force plate and Motion capture system (Vicon Nexus with 8 camera Bonita system) to validate the collected input data for the control system.

Both analog and video data were collected using the same experimental setup at the same time. A detailed explanation of the data collection methods using FFSs is discussed. Test rig parameters contain information about all of the symbols used in this thesis.

3.1 Model Development

The ErgoSkeleton is an idea that serves the purpose of assisting the lower back while lifting heavy loads. The ErgoSkeleton is a powered LAD that can be used during

lifting and material handling tasks by providing the required assistance to get the task done.

Figure 7 shows the Dynamic Model of the human body while the user is lifting the load. First, we studied the model. This model is used in the control system to estimate the torque.

The torque required to provide assistance to the user is given by[20]:

$$Estimated\ Torque = 0.5 * moment\ at\ (L5/S1) * 9.81 \qquad \text{Equation (2)}$$

$$Moment\ at(L5/S1) = ([UBW * L] + [\ W * h]) \qquad \text{Equation (2.1)}$$

here,

Ɵ is the torso angle from the horizontal,

α is the hip angle from vertical,

L is the distance from L5/S1 to the center of upper body (UPB),

h is the horizontal distance from L5/S1 to the load in hand (HD),

Fz is the ground reaction force,

W is the load in hand of the user and

UBW is the upper body weight of the user.

Using Equation (2) an estimate of the total torque required to provide assistance for supporting the upper body is determined. In the control system a DC motor and a torsion spring are used in parallel to provide the required level of assistance. Spring pre-load can be changed according to the bodyweight and load in hand of the user. The motor and spring parameters were derived by considering 50 percentile of male anthropometry

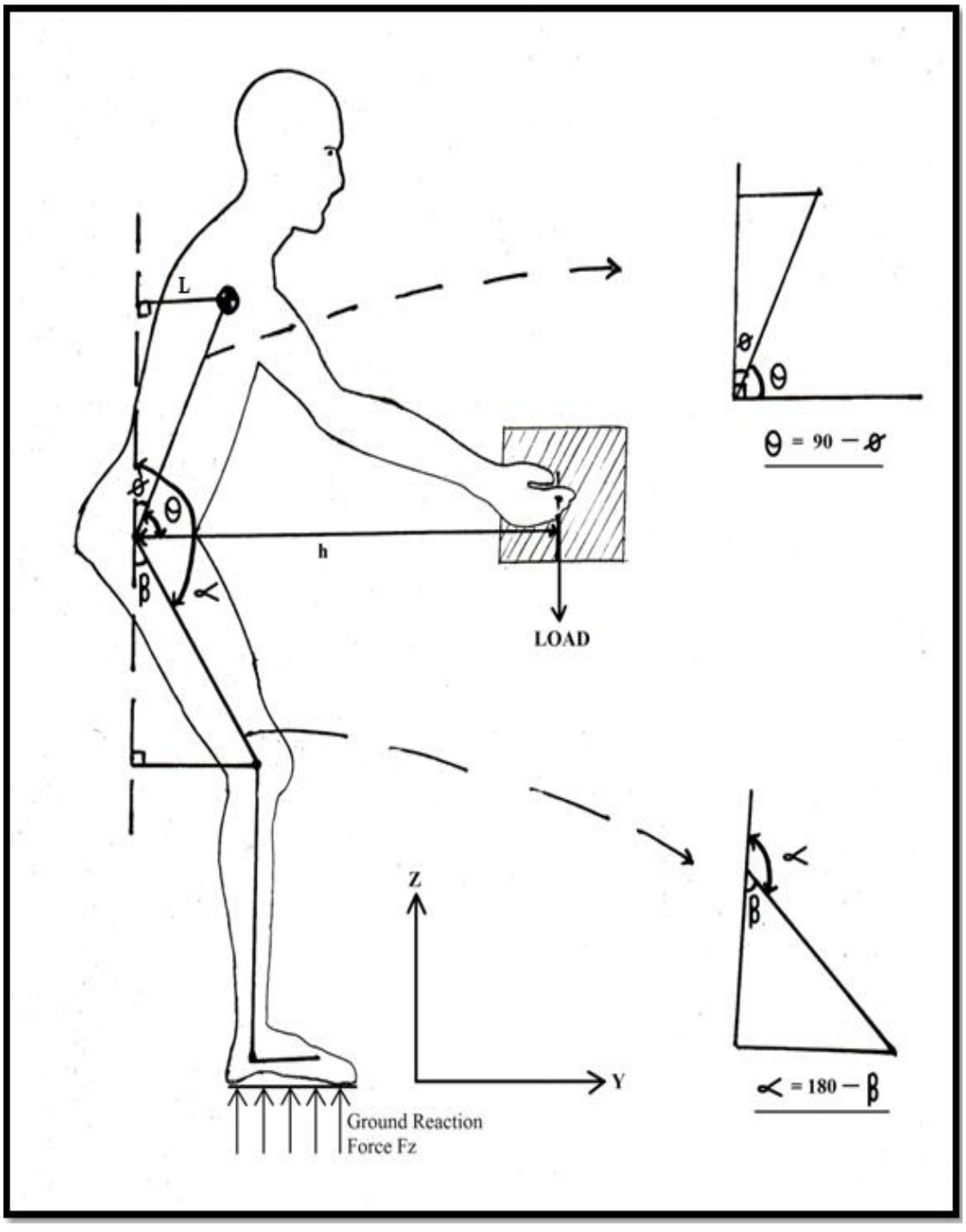

Figure 7 Dynamic Model of Human Body While Lifting the Load

data to provide assistance. The basic spring Equation (3) was used to derive the spring constant (k) value.

$$\tau_s = k * \alpha \qquad \text{Equation (3)}$$

here,

τ_s = torque from the spring;

k = spring constant;

α = hip angle

Now, the torque estimated from the Dynamic Model and the torque generated from the spring was used to calculate the amount of torque to be controlled by the controller to provide assistance to the user from the DC motor. The calculated total torque was sent to the control system to provide the amount of assistance to the back muscle for lifting and similar tasks. On the control system and on the physical model the arrangements were made to adjust the spring load based on the weight variation of the user's body. From the dynamic model using the ground reaction force and displacement in the y direction, the center of pressure was calculated to estimate the position of the load in the hand and to detect the amount of load in the hand.

3.2 Control System

The control system deals with the dynamic performance of the lifting assist device. There are two types of control systems, open loop control system (Figure 8) and closed loop control system(feedback control system) (Figure 9).

With the closed loop control system, error (difference between input and output) is detected from the system using feedback devices such as sensors. The controller

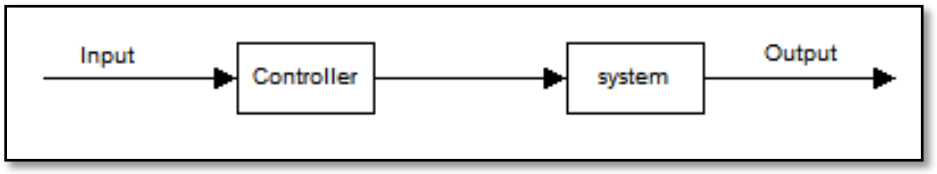

Figure 8 Open Loop Control System

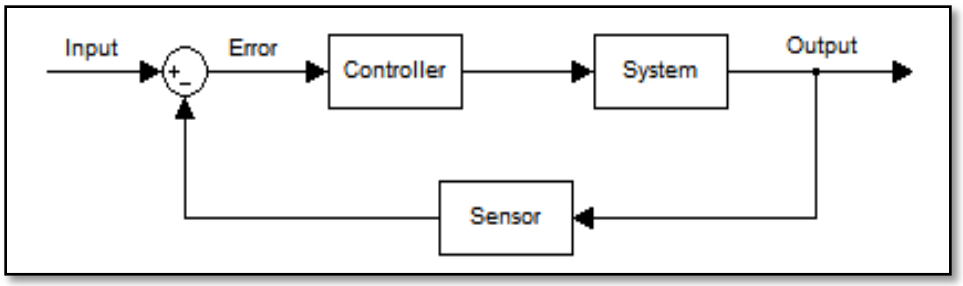

Figure 9 Closed Loop Control System

controls the parameters to achieve the desired output according to input. For getting precise system performance a closed loop control system was implemented. Concentrating on controlling the major parameter (torque), a torque control system was implemented.

3.2.1 Torque Control System

Using the torque control system, torque was controlled by current. From the basic equation of a DC motor, there was a direct relation between current and torque.

$$\tau_m = k_t * i \qquad \text{Equation (4)}$$

here,

τ_m= motor torque;

k_t = torque constant;

i= current supplied to the motor

Using Equation (4), according to the torque value the amount of current to supply the DC motor was determined by the controller. There are different types of controllers such as Proportional controller, Proportional and Integral controller and Proportional, Integral and Derivative (PID) controller. A PID controller was implemented to drive the DC motor.

3.2.2 PID Controller

A proportional, integral and derivative controller (Figure 10) is a general feedback control system that is the most common controller used for this type of feedback control application. The feedback control system measures the error difference between given processed value (output) to the desired set point value (input) [21]. The controller tries to minimize the error depending on the gain values.PID controller has three different gains Kp for proportional, Ki for integral and Kd for derivative term.

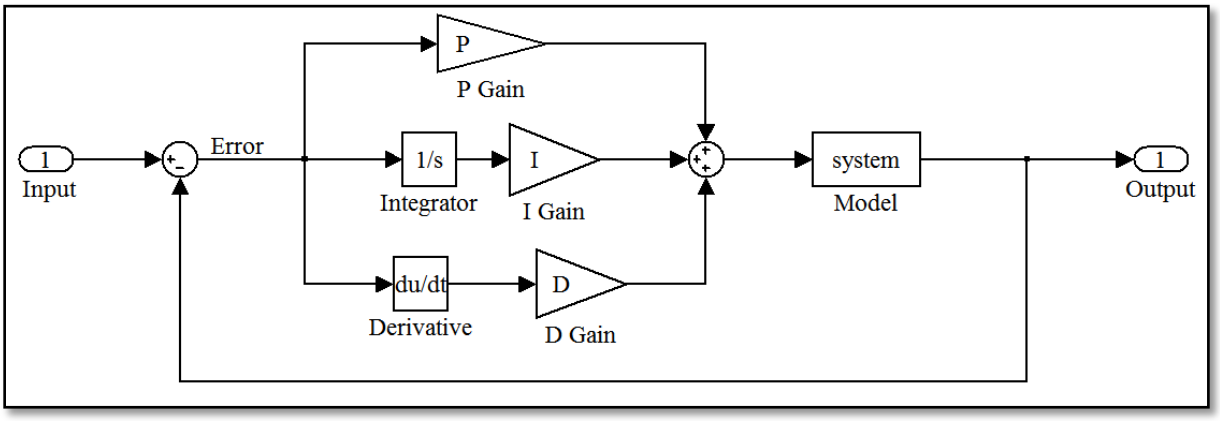

Figure 10 A Block Diagram of a PID Controller

All these gain units were amp/N.m based on our controller input (torque) and output (current).

The effects of each gains on the system are, for proportional controller (Kp) reduces the rise time. An integral control (Ki) has the effect of eliminating the steady-state error, but it can make the transient response worse. A derivative control (Kd) has the effect of increasing the stability of the system, reducing the overshoot, and improving the transient response[22]. Since in this study a virtual control system was adopted, PID was the best choice but on the real device it might not give the same performance because of external noise, system nonlinearity and other disturbances.

Figure 11 shows a block diagram of the designed Ergoskeleton control system. The block diagram is the basic working cycle of the simulation. This control system is developed under Matlab software in Simulink. The control system is divided mainly into three parts:1) Dynamic Model calculation, 2) Controller block including PID controller and3) dynamic model of the DC motor.

From the Dynamic Model, the estimated required total torque values to provide the assistance to the body were calculated. The total torque using Dynamic Model was calculated by using the input parameters as torso angle and HD (Horizontal Distance from L5/S1 to center of load derived from the Force and COP using Flexi Force Sensors in the shoe insole) of the system. Calculation of the input parameter is discussed in a later section. First, running the Dynamic Model the maximum torque and speed requirement was derived.

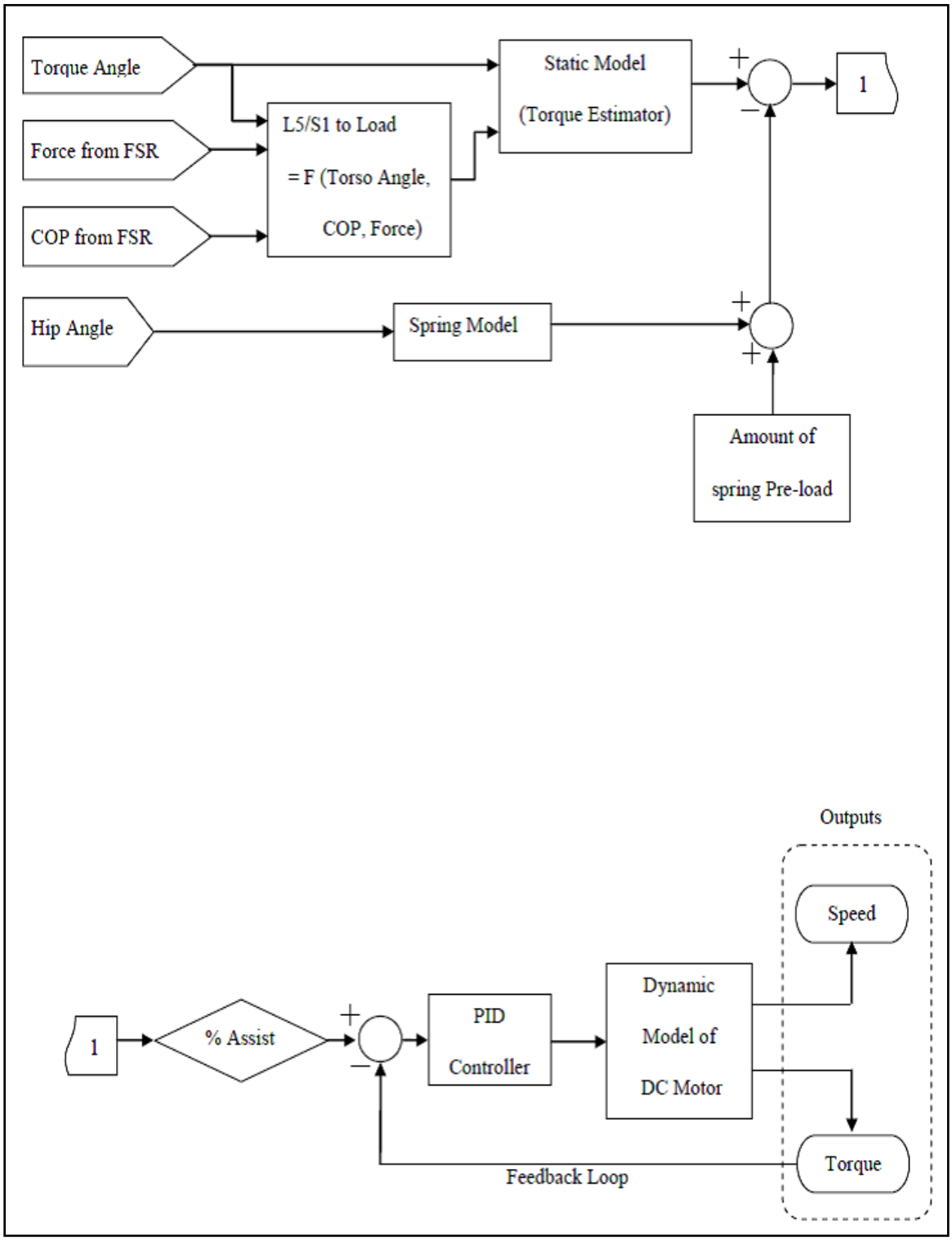

Figure 11 Flow Diagram for Control System of Assist Device

Based on the torque and speed requirement and amount of voltage and current were calculated which can be feasible to provide to run the motor. All together a DC motor with specific motor dynamic parameters was selected. The parameters are as shown in Table 1. On the developed control system required motor parameters were fed as a value. To measure the control system output parameters, the mathematical equations were derived for the entire control system. The logic of the control system is attached in form of Pseudo Code in the Appendix.

3.3 Data Collection

Data were collected using the setup shown in Figure 12. In this setup PC, A/D converter (NI Data Acquisition Box), power board with 4 I/P and 4 O/P channel pins, force plate (AMTI Model OR6-7-1000) and a customized shoe sole placed on four FFSs were used as hardware. Under the motion capture system using the setup shown in Figure 12, the data were collected at 1000 Hz frequency.

PC was used to store all data from the hardware via A/D converter. A custom made shoe sole with four FFSs placed at different locations was used. These FFSs were placed on the force plate to collect force values from the FFS in the form of voltage and force values form the force plate at the same time.

Table 1 DC Motor Specification

DC Motor Specification			Unit
Inductance	L	0.0137	H
Torque/Current Constant	Kt/Kphi	0.1157	V/rpm
Total Inertia	J	13.4100	Kg.m.s²
Friction/Damping Co-efficient	b	0.3300	N.m.rad/s
Resistance	R	1.2800	Ω

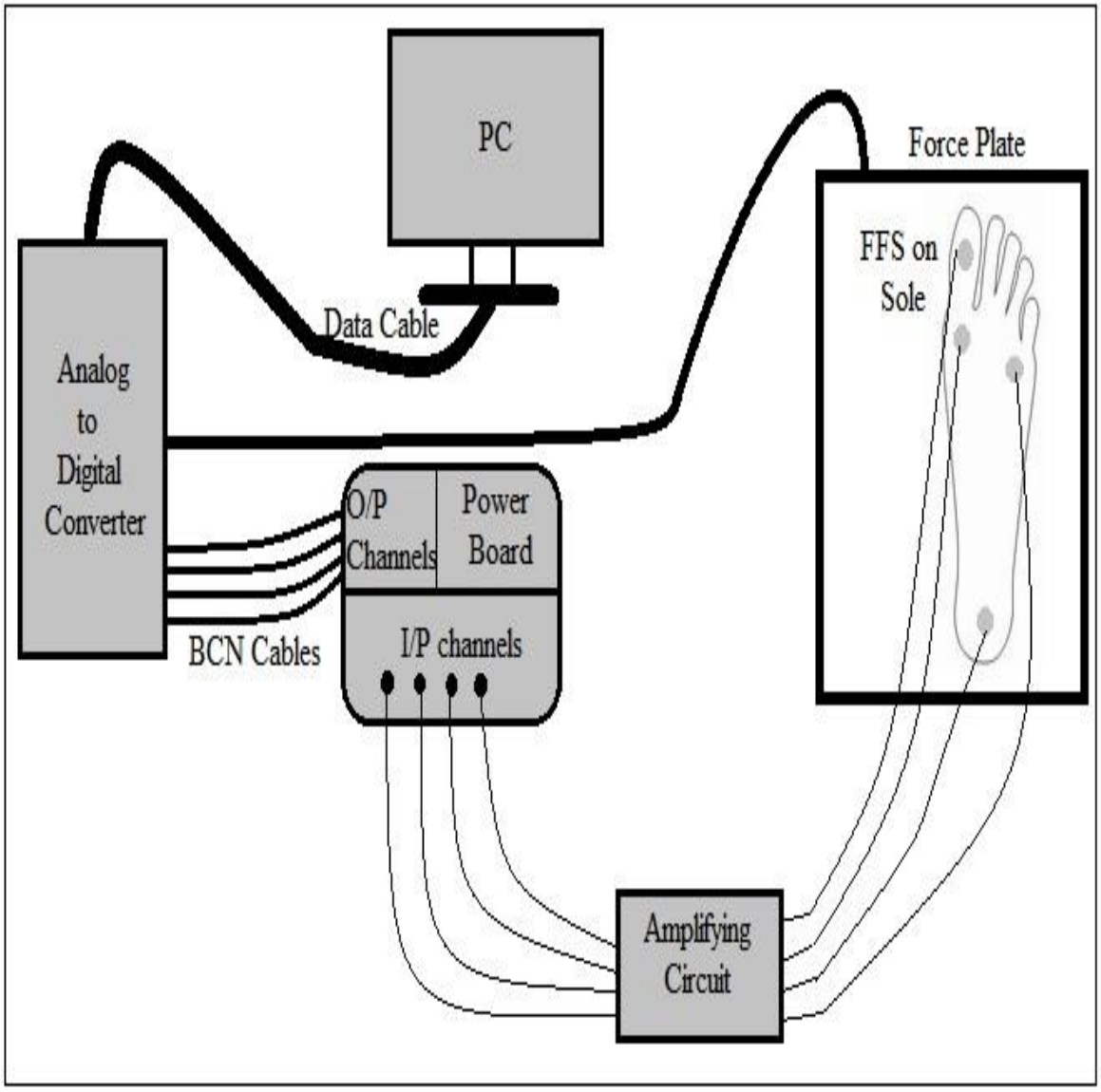

Figure 12 Setup for Collecting Data for Lifting Trials

FFSs were connected to the amplifying circuit to amplify the voltage signal to make the data readable. Four FFSs were powered using a customized power box with 12v supply. The power box has 4 I/P and 4 O/P channel pins to run the FFS output data to the A/D converter. Force plates were also connected to the A/D converter. Vicon Nexus software was used to store all the digital output data from the A/D converter. Using this setup, data were collected for various lifting trials and processed in the Matlab.

3.3.1 Motion Data

The data were collected using an 8 camera Bonita system and Vicon Nexus[23]. Motion capture data were collected to use in the simulation and compare with calculated results from the control system. The lifting trials were conducted with the motion capture system using the plug-in-gait marker template[24] to connect the body segments (Figure 13). Thirty Six reflective markers were placed on the body to capture the movement.

Using the markers' location data, required parameters were calculated including angles and moment. In Matlab software using Equations (5, 6 &7) torso angle, hip angle and HD were calculated. The HD data were used to validate HD calculated by the predicted function (Equation (9) discussed in later section).

$$\theta = 90 - \left(\tan^{-1} \frac{\left(RSHO_Z - \frac{RPSI_Z + RASI_Z}{2}\right)}{\left(RSHO_Y - \frac{RPSI_Y + RASI_Y}{2}\right)} * \frac{180}{\pi} \right) \qquad \text{Equation (5)}$$

$$HD = \left(RFIN_Y - \frac{RPSI_Y + RASI_Y}{2} \right) \qquad \text{Equation (6)}$$

$$\alpha = 180 - \left(\tan^{-1} \frac{\left(\frac{RPSI_Z + RASI_Z}{2} - RKNE_Z\right)}{\left(RKNE_Y - \frac{RPSI_Y + RASI_Y}{2}\right)} * \frac{180}{\pi} \right) \qquad \text{Equation (7)}$$

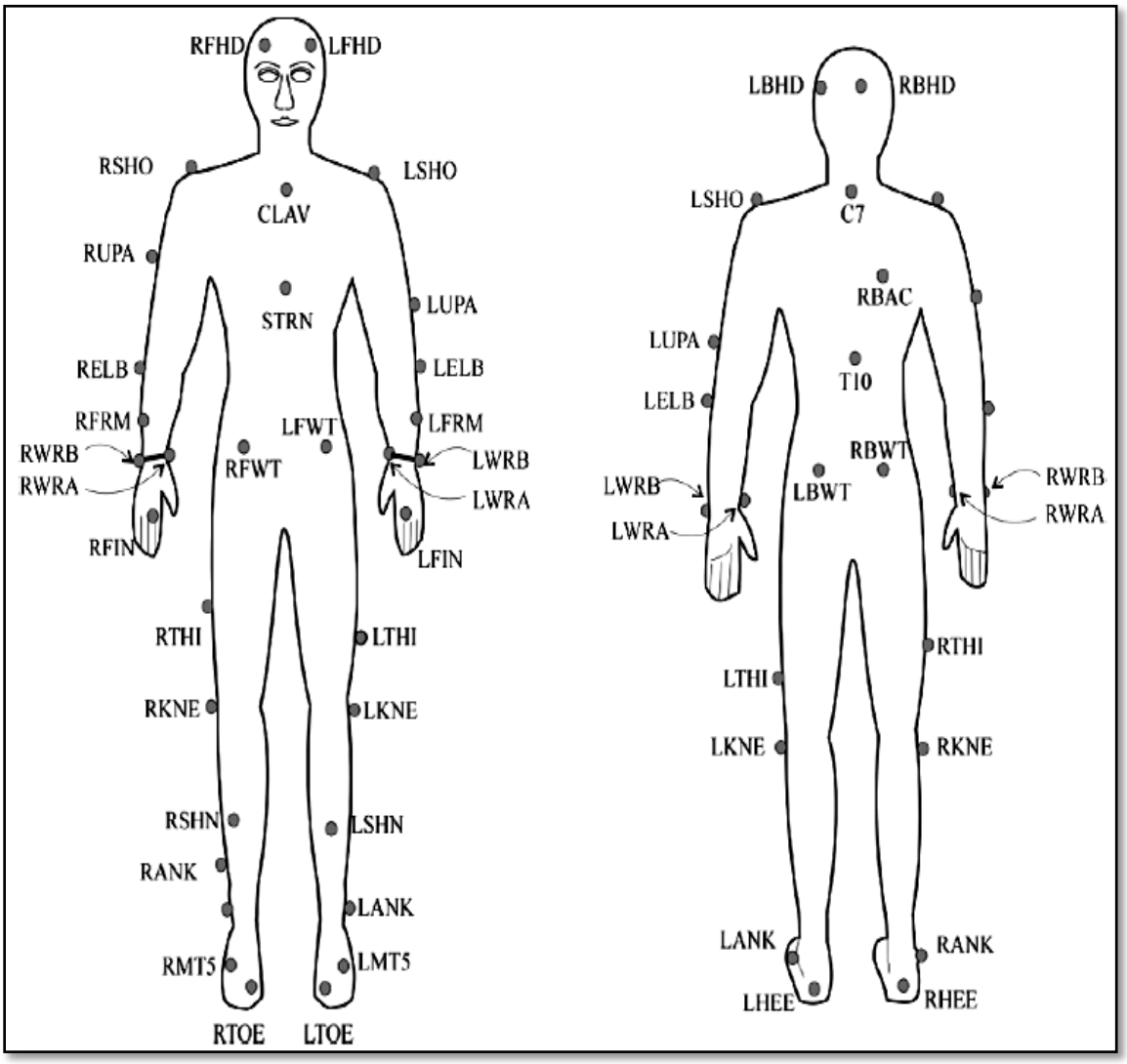

Figure 13 Template for Plug-in-gait Marker Placement

3.4 Method of Deriving Input Parameters

Parameters were collected from the test setup discussed in Figure 12. But the major input parameters for the control system like Force from FFS and HD could not be derived directly from the experimental setup. In following sections the method to derive force data from FFS and HD parameters are discussed in detail. For HD data COP from

FFS was used. So, the method to calculate the COP is also discussed. Before that, brief information on the FFS is given.

3.4.1 Flexi Force Sensors (FFS)

The FFS in Figure 14 are used to measure force in static and dynamic conditions. They are capable of measuring up to 1000 lbs. These sensors function on a resistive-based technology. The ultra thin sensors manufactured using flexible printed circuit are used to measure force between two surfaces [25].

3.4.1.1 Construction of FFS

The sensors are constructed of two layers of substrate. This substrate is composed of polyester film. On each layer, a conductive material is applied, followed by a layer of pressure-sensitive ink [26]. Adhesive is then used to laminate the two layers of substrate together to form the sensor. The silver circle on top of the pressure-sensitive ink defines the “active sensing area” which is 0.375” in diameter

3.4.2 COP from FFS

Center of pressure is the point on the surface where the sum of all the forces acts, causing a force but no moment [27]. In this case, while in standing position, the forces exerted by the foot on ground can be determined using Flexi Force Sensors (FFS) beneath the feet. There are two types of forces generated. One is the normal force and the other is frictional or shear force.

Figure 14 Flexi Force Sensors (Copyright © 2007 Tekscan, Inc.)

Reprinted with Permission

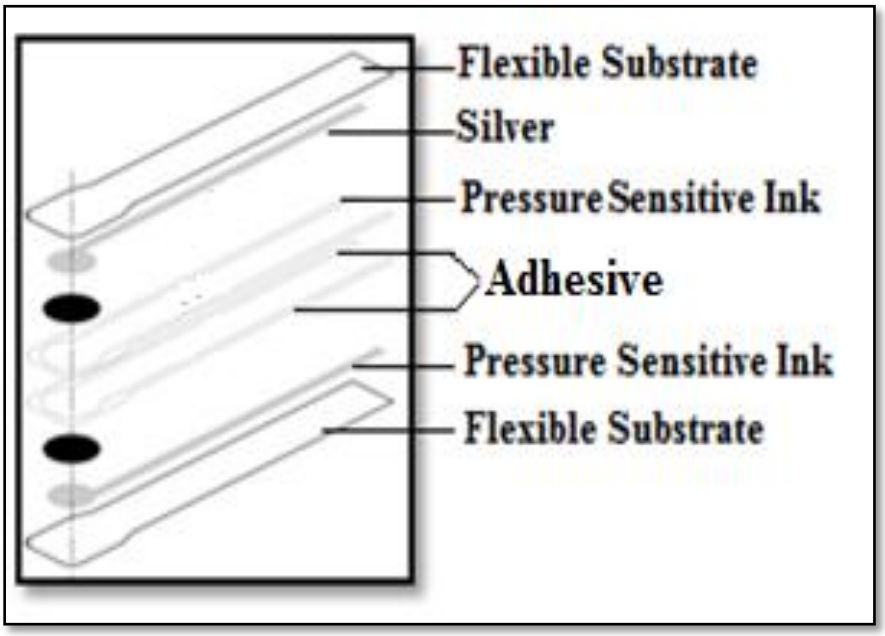

Figure 15 Construction of the Flexi Force Sensor (Copyright © 2007 Tekscan, Inc.)

Reprinted with Permission

Considering there is no sliding of the foot on the ground surface during the expected lifting scenarios, the friction force will be ignored and set to zero [28]. For calculating the COP values, a customized insole with four FFS to get the force profile data was used. Depending on the variation in the force values of FFS, the COP was calculated at each movement of the user's body. In this study for validating the COP from FFS COP from the force plate was used.

After getting the force data from FFS, the COP was estimated. Now for the COP data, considering that both the foot are in symmetry so, the outcome must be same from the left and right foot. Thus data from only the right foot were considered in further study. Now using data from one foot COP was calculated in anterior/posterior direction using Equation (8) which was already derived from a previous study[29]. In Equation (8), *X* is the location of each FFS on the shoe sole, *Fi* is the force from the FFS and *αi* is the weighting factor which is used to get more accurate and precise values.

$$COP = \frac{\sum_{i=1}^{n} \alpha i Fi Xi}{\sum_{i=1}^{n} \alpha i Fi} \qquad \text{Equation (8)}$$

Figure 16 shows the exact positions (*Xi*) of each FFS on the shoe sole. Force values were calculated using calibration equation as shown in section 3.4.2.1.

The weighting factors were derived using a nonlinear least square method by comparing the force data from FFS and force data from the force plate [29]. Finally the relation was established between the COP values from FFS and COP from force plate to validate the COP results from FFS.

3.4.2.1 Calibration method for FFS

Calibration is the method by which the sensor's electrical output is related to an actual engineering unit. Actually these flexi force sensors give output in terms of voltage. For deriving the relation between force and output voltage, the same force plate was used.

The calibration task for each FFS was performed. First the FFSs were placed on top of the force plate and using Force dynamometer (Chatillon® DMG Series Ergonomic Gauge) force was applied on each FFS at the sensing area in a range from 0 to 150 lbs in

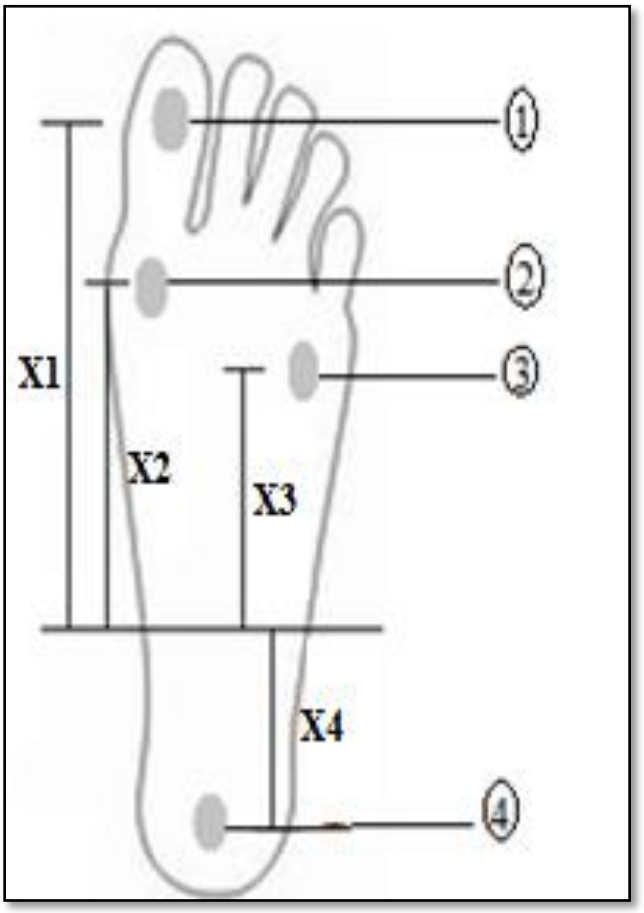

Figure 16 Each Sensor Location on Shoe Sole

consistent increasing pattern until applied force reached to 150 lbs. The same procedure was performed to remove the applied force down to zero for each FFS. After getting both datasets from the force plate and voltage from the FFS, a plot of the data for each FFS in terms of voltage v/s force was derived.

Using a curve fit method the trendline was assigned by 3rd and 4th order Polynomial equation for each dataset. As shown in Figures 17 and 18, proper fit were achieved where the values were between 0.98 and 0.99 for all FFS. Now, using these equations the force values were calculated from the voltage generated by FFS.

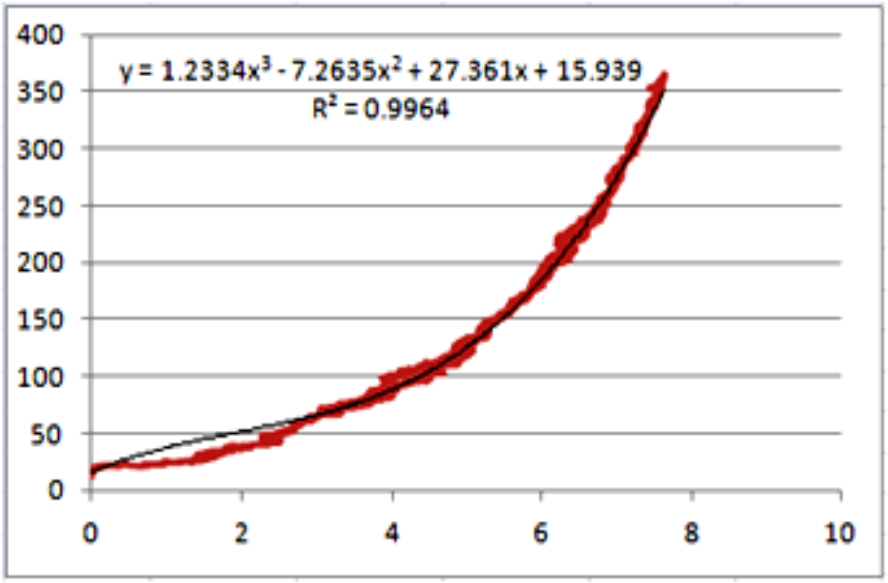

FFS - 1

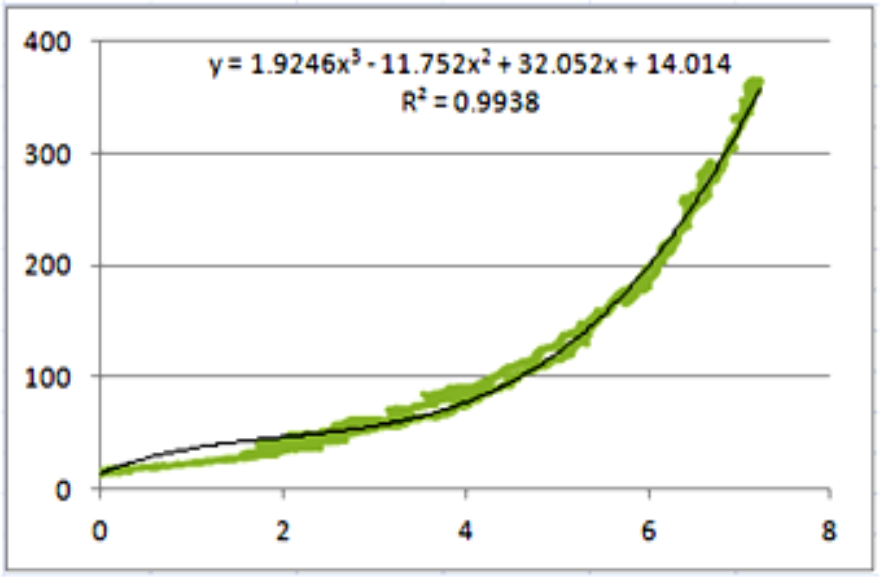

FFS - 2

Figure 17 Flexi Force Sensor Calibration Voltage (V) v/s Force (N) Plots

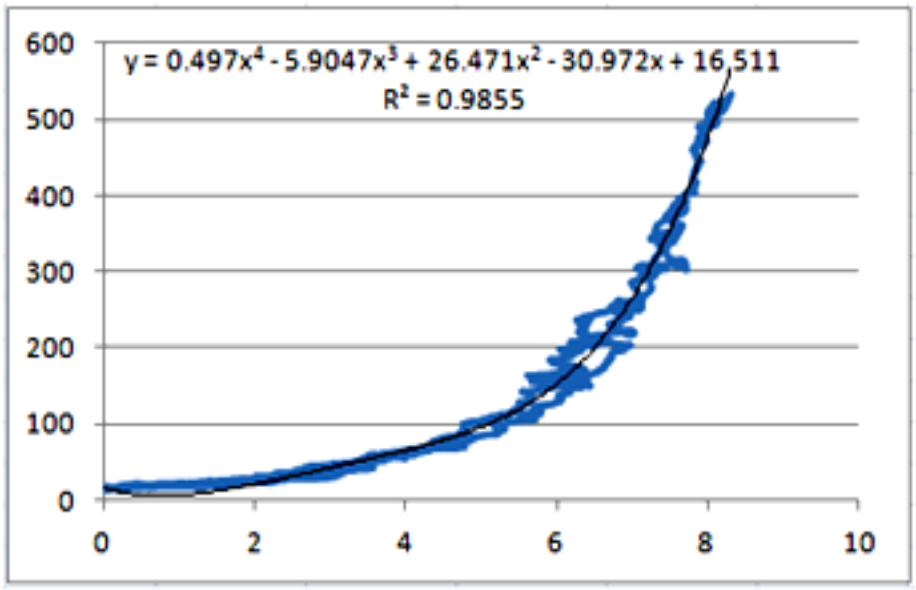

FFS - 3

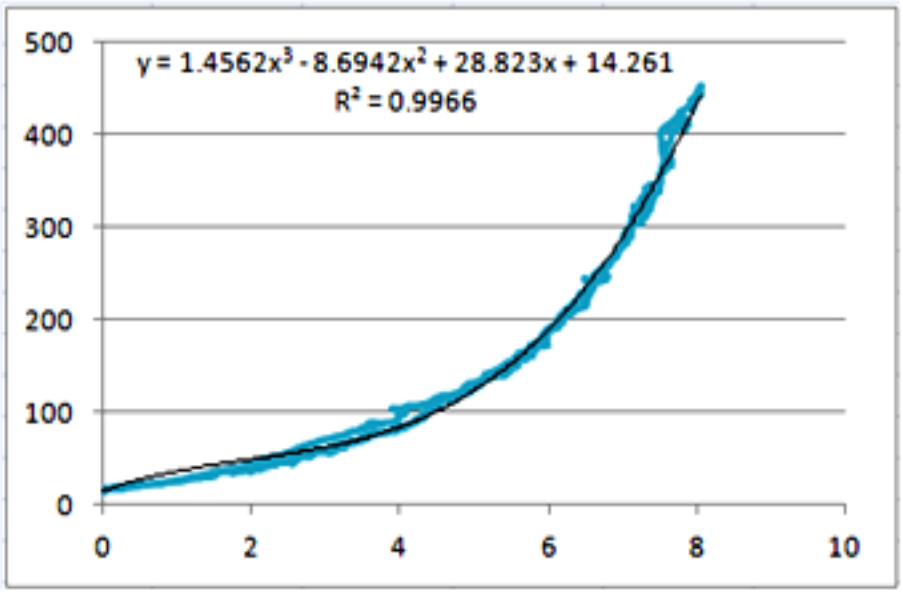

FFS - 4

Figure 18 Flexi Force Sensor Calibration Voltage (V) v/s Force (N) Plots

3.4.3 Horizontal Distance (Distance from L5/S1 to Load in hand)

Horizontal Distance (HD) is one of the main parameters required for a properly working control system. This parameter gives the location of load in hand from L5/S1 in horizontal. As shown in Equation (2.1) it was a large contributor in generating required torque based on the Dynamic Model (Figure 7).

To derive this parameter, a function was created in terms of force from FFS, COP from FFS and torso angle. For creating the function, a linear regression method was used with input x parameters as force, COP and angle and HD from force plate as an input y parameter. From the regression results β values, error (ε) and R^2 value with 0.9069 were achieved. Table 2 shows the regression results.

In Table 2 from the regression values we determined the equation for predicting HD is:

$$Y = (\beta_1 * X_1) + (\beta_2 * X_2) + (\beta_3 * X_3) \pm \varepsilon \qquad \text{Equation (9)}$$

Table 2 Data from Regression for HD

R^2 Value		0.9069
β Values	Force from FFS - β 1	-4.0224
	COP from FFS - β 2	5.8025
	Torso Angle - β 3	4.5985
Error–ε		365.5323

here,

Y = Predicted Horizontal Distance,

X_1 = Force from FFS,

X_2 = COP from FFS and

X_3 = Torso Angle.

Using the β values as co-efficient factors and the error (ε), by substituting values in Equation (9) predicted HD was derived. All the test rig parameters which were used in this study are shown in Table 3.

Table 3 The Test Rig Parameters for Control System

Symbol	Unit	Description
τ	N.m	Torque
τ_m	N.m	Motor Torque
τs	N.m	Spring Torque
Kt	N.m/amp	Torque Constant
K	N.m/rad	Spring Constant
i	amp	Current
Θ	deg	Torso Angle
α	deg	Hip Angle
R	Ω(ohm)	Resistance
L	Henry	Inductance
b	N.m.rad/sec	Damping/Frictior_Coefficient
Kp	amp/N.m	Proportional Gain constant
Ki	amp/N.m	Integral Gain constant
Kd	amp/N.m	Derivative Gain constant
Fz	N	Ground Reaction Force
h	mm	HD (Horizontal Distance from L5/S1 to Load in hand)

4. RESULTS AND DISCUSSION

This chapter presents results and discussion of the parameters of the control system performance. Results give determination for the working of the control system by providing outputs from reliable input parameters. In this section first the results from input parameters are discussed followed by statistical analysis results for hypothesis testing and last the output parameter results.

4.1 Input Parameters

4.1.1 Force andCOP

For simulation of the control system, initially force and COP were calculated from FFS. A comparison was made between the calculated values from FFS and the data collected from the force plate. Before analyzing the COP data, it is important to analyze the force values from FFS and force plate. We observed the trend between force data from FFS and force plate data shown in Figure 19.

There is a significant difference between both the forces, which is constant for all data points. This difference comes from the force measuring device. Now the same force data and sensor locations of each FFS from shoe sole are used to calculate COP using Equation (8).

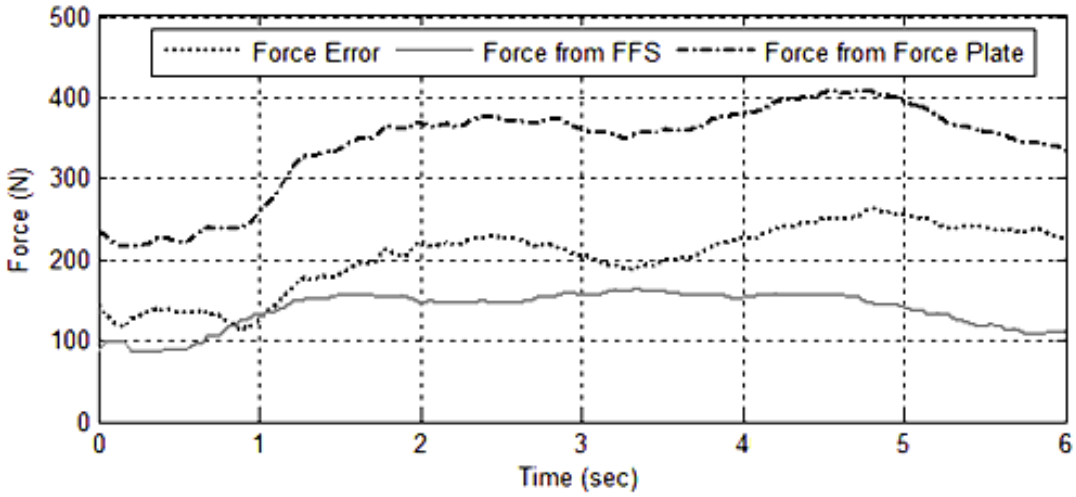

Figure 19 Force Comparison Between Force Plate and FFS

Therefore, the same constant difference is going to reflect on the COP data because the COP values are derived using the same force values. For analysis, COP data were calculated only in an anterior/posterior direction (y-direction as in Dynamic Model Figure 7) conducting a leaning trial. In Figure 20, COP data from force plate and calculated COP data from FFS force data are shown for two lift cycles. As said before, the difference in data is because of the FFS performance and very low saturation point of the FFS. So, that the sensors were saturating oftentimes. One more reason with FFS for not achieving the better result is these FFSs are very thin in structure and the sensing area is too small. Also, the foot surface profile is not flat and it is hard to collect all the ground reaction force values at each contact point using only four sensors. Using more precise technique much better results could be achieved, but at the same time the cost of the setup would go higher.

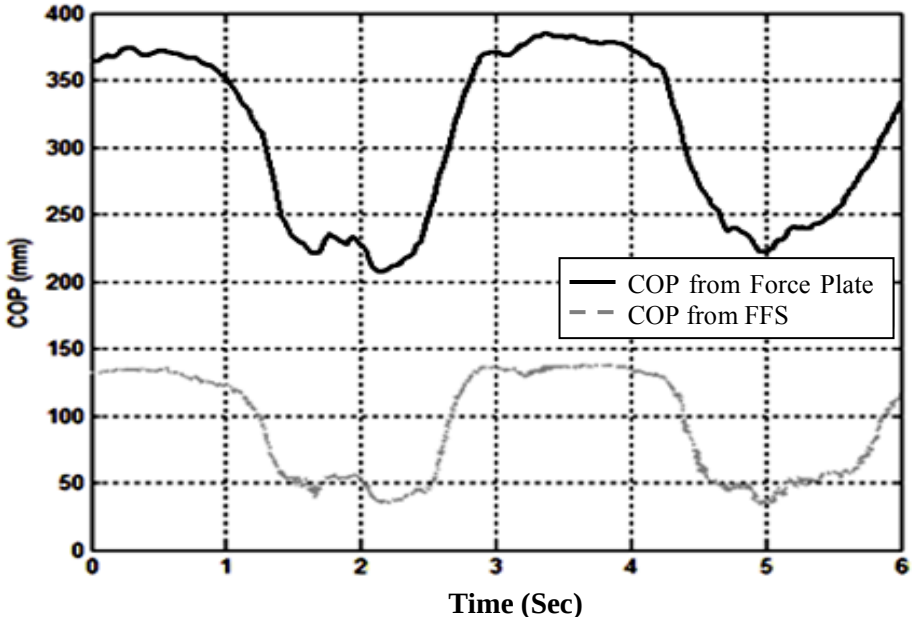

Figure 20 COP in the Anterior/Posterior Direction (Y-Direction as in Dynamic Model Figure 7) From Force Plate and FFS

4.1.2 Horizontal Distance (Distance from L5/S1 to Load)

To predict the horizontal distance (HD), four major parameters have been used. Force data from FFS, COP data from FFS and torso angle data are used to find the predicted HD using created function. The HD data are validated by HD derived directly from motion capture system using Equation (6).From all three parameters, COP has the greatest influence on the predicted HD with the co-efficient (β value) of 5.8025 shown in regression Table 2. In Figure 21, experimental and predicted HD variables are plotted and reasonable consistencies with the data were observed. Plot for % error in predicted HD has ±20% error from the experimental data, though this appears to be acceptable. The error comes from marginal FFS performance. To reduce the error to a very negligible amount, force data can

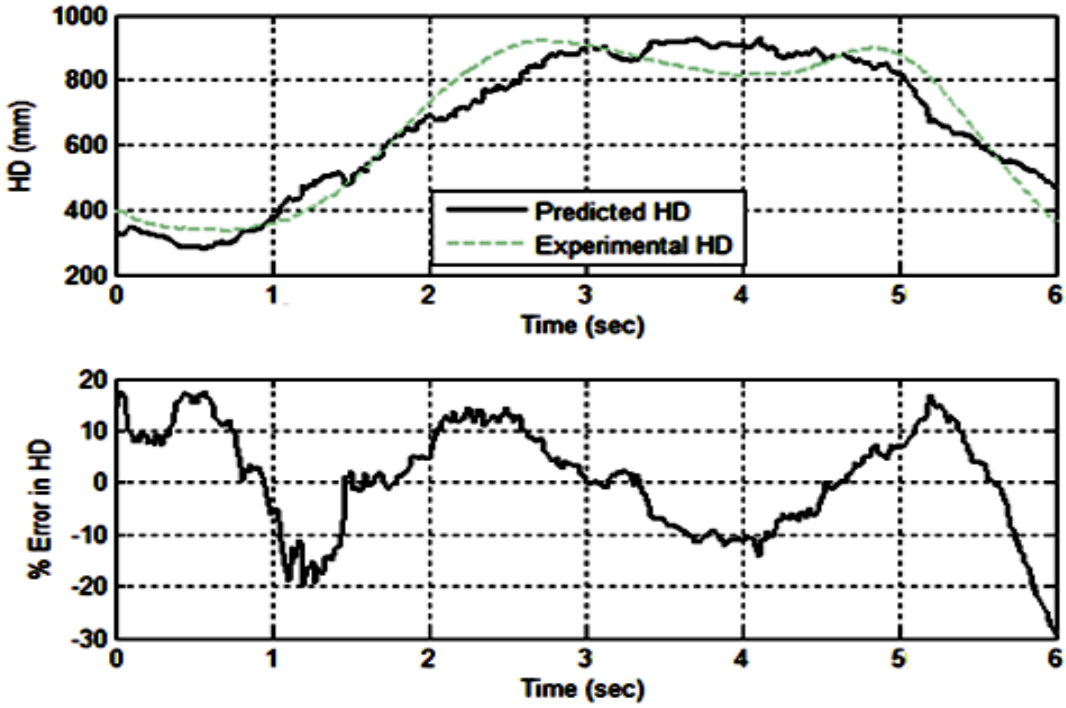

Figure 21 Comparison of HD from Experimental and Predicted and % Error

be improved by using more precise load cells or miniature force sensors as a replacement of the FFS. The FFSs served their purpose to the system by providing reasonable results at a low cost. Even using these less desirable data, we seem to be successful in achieving our goal for the study.

4.1.3 Statistical Analysis

Different types of lifting data were used for performing statistical analyses. For statistical comparison and evaluation, the Bland Altman method was used to verify the relation between data sets. First we performed the analysis using the Bland Altman method to find out the significant relationship between HD data derived from motion capture data using Equation (6) and HD data calculated using predicted function (Equation (9)). Figure 22 shows result of performed analysis on the HD data.

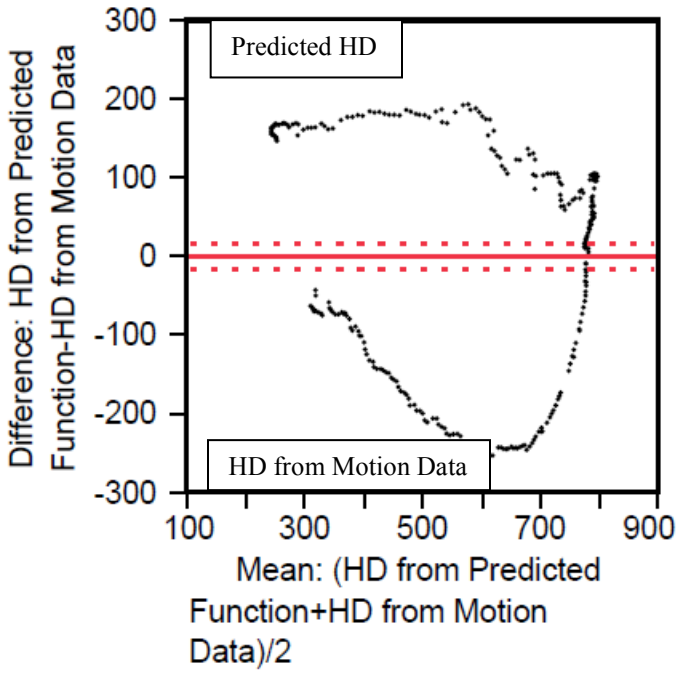

Figure 22 Data Comparison of HD Data Between Predicted Function and Force Plate Using Bland Altman Method

In the plot, HD data from the predicted function and HD data from force plate are compared. The statistical analysis result revealed that both the values are significantly equal with p=0.9868 and mean difference of between the data is very close to zero, which is -0.1403 mm. So, the hypothesis has been accepted by saying both the HD values are equal. Using the same method, statistical analyses have been performed for COP and force data, collected from the force plate and calculated from FFS. Data comparisons for the force data and COP data are shown in Figure 23 and Figure 24, respectively.

From the statistical results the p-values is less than 0.001 and the mean difference value is -172.39 mm, which shows that the difference between the sample values of both method is very big.

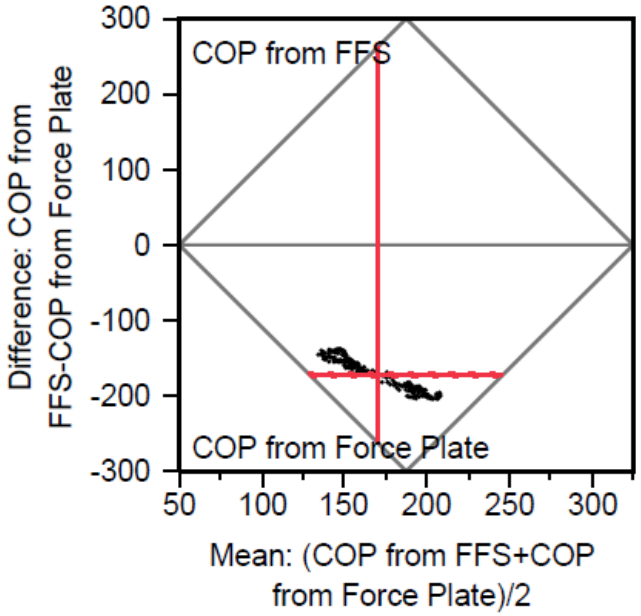

Figure 23 Data Comparison Between COP Data Calculated from FFS and Collected from Force Plate Using Bland Altman Method

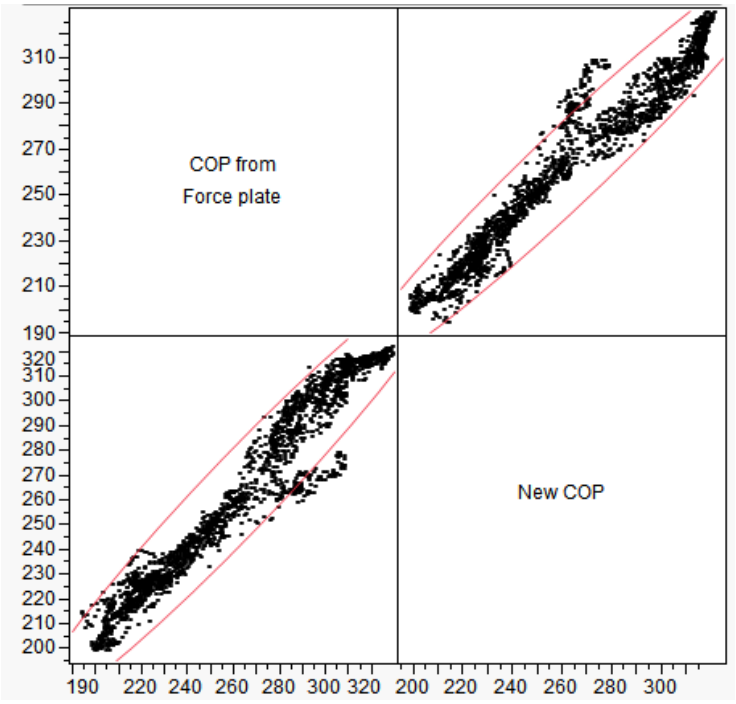

Figure 24 Spearman's Method for COP

From the results second hypothesis has been rejected which shows that both the COP values are significantly different. The same behavior was previously observed in the COP comparison shown in Figure 20.

Using Spearman's method COP values are compared again to find out the correlation between new COP values which is re-calculated using weighting factors and constant error. Table 4 shows the weighting factor values from regression values.

Substituting the derived weighting factors the new COP was calculated. As Figure 24 shows, the statistical analysis was performed using both the COP values to find out the correlation between both the values. The correlation value from Spearman's method was 0.9715, which shows strong correlation for both the data set for same parameter values.

In Figure 25, similar results were obtained for force data from different methods and the result shows that the values are significantly different with $p<0.001$ and the mean difference is as big as -245.14 N. From the statistical results, the third hypothesis can also be rejected indicating both force values are not equal derived from different method. A more comprehensive check of variation between the force values was done using regression to detect the constant error of the device used to calculate the force.

Table 4 Weighting Factor Values

Weighting Factors	α_1	α_2	α_3	α_4
	2.7412	5.9317	1.4289	2.5017

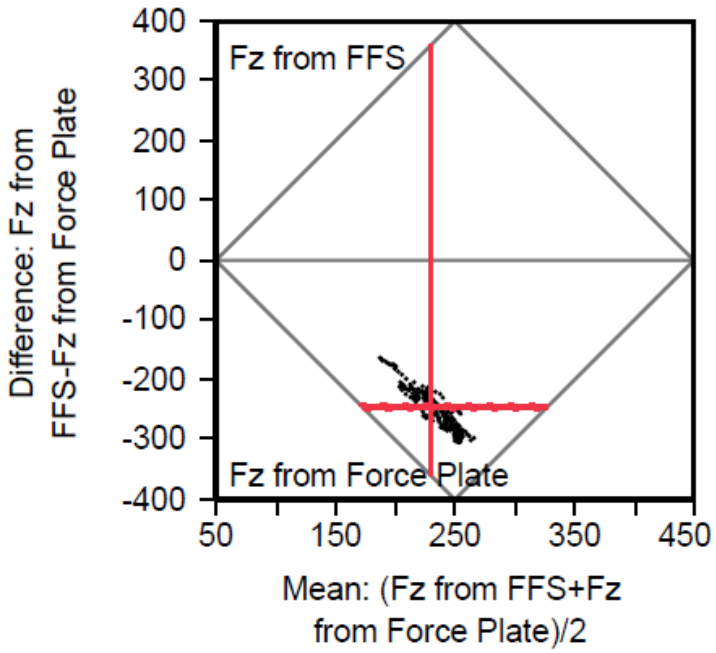

Figure 25 Data Comparison Between Force Data Calculated from FFS and Collected from Force Plate Using Bland Altman Method

The linear regression method was performed on the force values to derive the constant error (Table 5) to correct the values obtained from the force measuring device (FFS).

The new force data were calculated by adding the constant error term and the resultant force value was recalculated. Again using Bland Altman method, both the force values (force from force plate and recalculated force from FFS by adding constant error) were compared and are shown in Figure 26.

Table 5 Constant Error in Force from FFS Derived Using Regression Method

Constant Error	160.8682

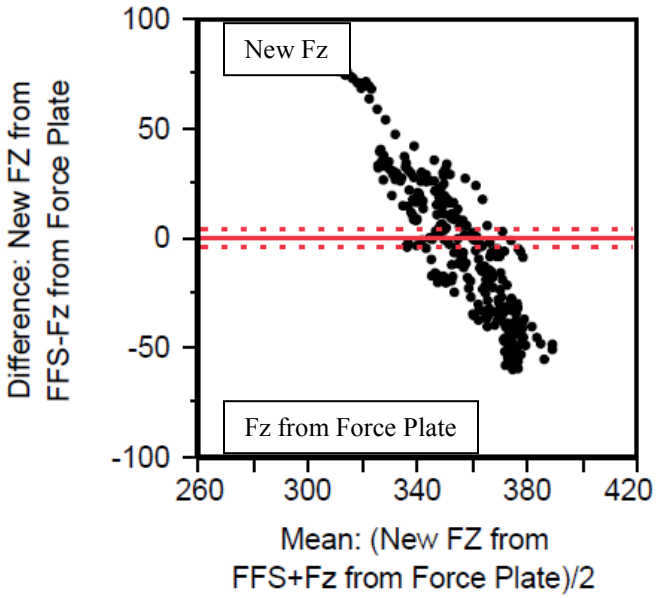

Figure 26 Data Comparison Between Re-calculated Force from FFS and Collected Force from Force Plate Using Bland Altman Method.

This analysis was performed to make sure the derived FFS error was minimized. The analysis results are very convincing and show that both actual and calculated force values are now equal.

The analysis report also indicates the *p*-value is 0.997 and the mean difference is almost zero (-0.0077 N). From this analysis it can be concluded that the largest force difference originally identified exists because of the error in device (FFS) used to measure the force.

4.2 Output Parameters

4.2.1 Torque, Speed, Torque Error and Current

The major outputs of the developed control system are torque and speed. A few lifting trials have been conducted with different postures to differentiate the results based

on the lifting postures. Using input parameters from physical lifting trials, simulations have been run for different lifting postures. These postures were semi-squat posture, stoop posture and squat posture to observe the output parameters.

Figure 27 shows the simulation results for two lifts using the stoop posture. The plot shows four output parameters which are torque, torque error, required current to run the motor and speed from the motor. The highest torque required and provided is around 56 Nm as shown in the plot. This torque indicates that the user is in a standing position with a torso angle close to 90 degrees from the horizontal. At this point the system is trying to push the upper body of the user in the anterior direction to maintain the neutral standing position by providing a negative torque. The negative torque can be eliminated by using a condition when the torso angle is greater than 85 degrees from the horizontal. Then, no torque should be generated by the motor and the user can freely stand. At the start of a lifting cycle, between 0 - 0.6 sec and between 5 - 7 sec the torque is negative. The reason behind this is the torso angle is close to 0 degrees from the horizontal.

The tracking error is small at ±1.25 Nm. There are two peaks at the start of the lift. These indicate that the motor and spring are engaging with each other at this point. The current requirement is between 8 to 9 amps, which is feasible to supply the amount of voltage to the system. Speed looks different for both lifting cycles. The reason is because it tries to reach its maximum speed with a constant supplied power source. This can be manipulated by changing the Kp gain, which directly affects the rise time. This also increases the operating speed range according to the motor speed limit.

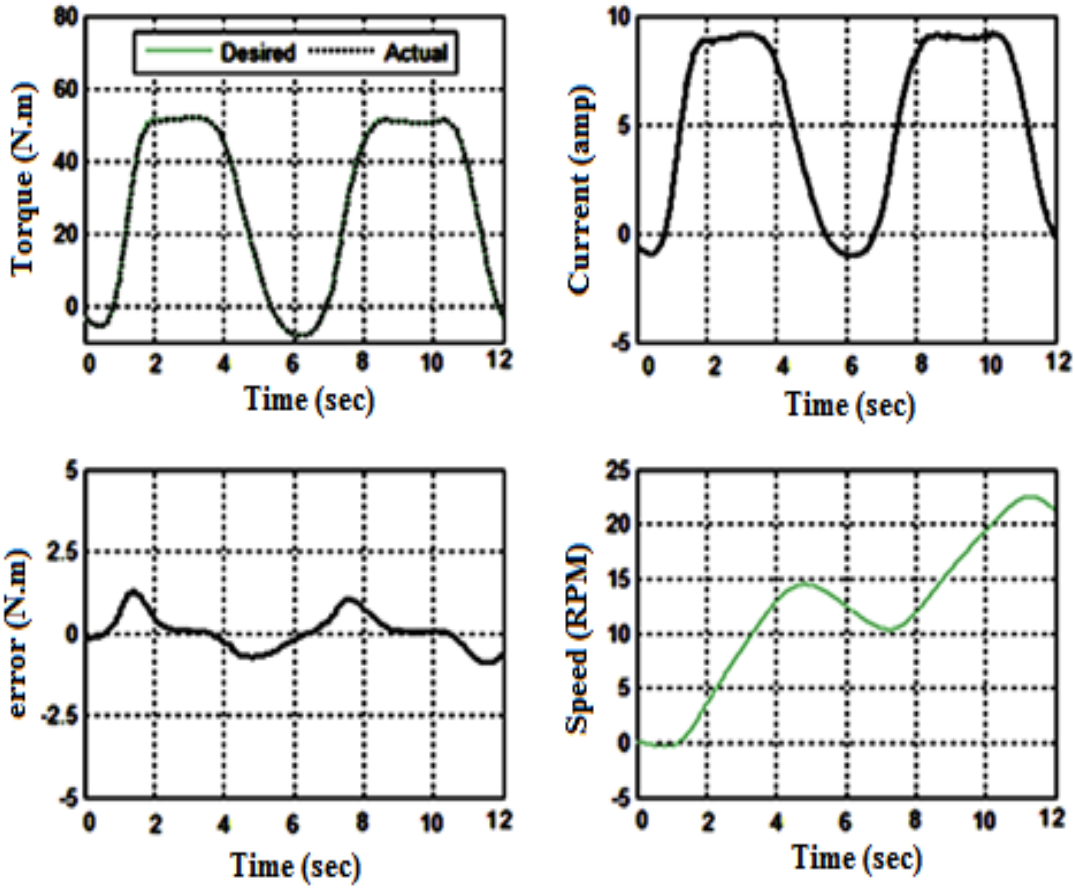

Figure 27 Outcome Parameters (torque, torque error, current and speed) of Stoop Posture Lift

Figure 28 shows the output parameters of two lifts from the squat posture. The torque outcome is lower than the stoop posture. In the squat posture the knees are always bent so there is less force exposure at the erector spine muscle while bending. There is very little torque error. Speed and current outcomes are also similar as in the stoop lift.

The data for the lifts in the semi-squat posture have not been discussed here but the results are very similar to both stoop and squat postures. It can be said that semi squat lifting posture is the combination of stoop and squat postures.

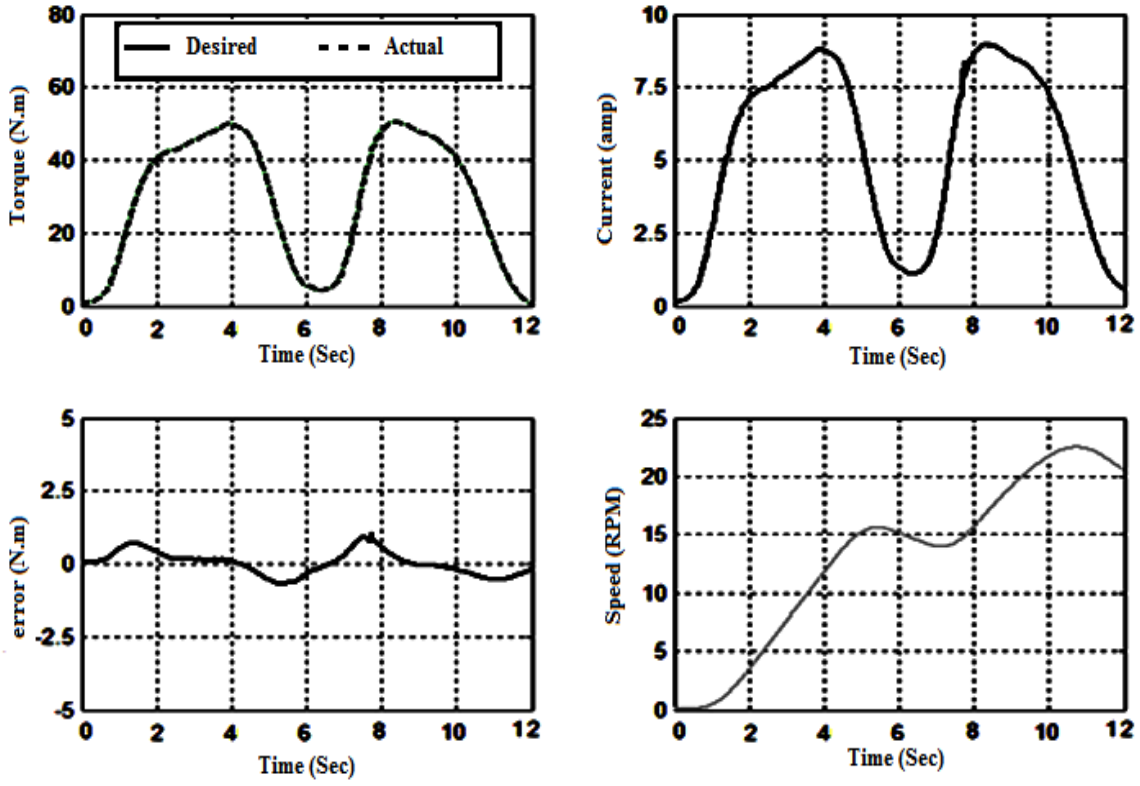

Figure 28 Outcome parameters (torque, torque error, current and speed) of Squat Posture Lift

All outcome parameters depend on motor parameters (Table 1) and PID gain values. These are the main controlling aspects of the system. Motor parameters help the system generate the amount of torque the system is required to provide to the user. PID gains take care of the performance of the system according to the system error.

Figure 29 illustrates torque comparisons between two different lifting trial datasets. From the plot, different torque requirements are easily visible. Here the torque requirement seems higher for squat than stoop, which is different from Figures 27 and 28. With a typical stoop posture at the fully flexed position, the user requires more support in terms of torque compared to a squat lift.

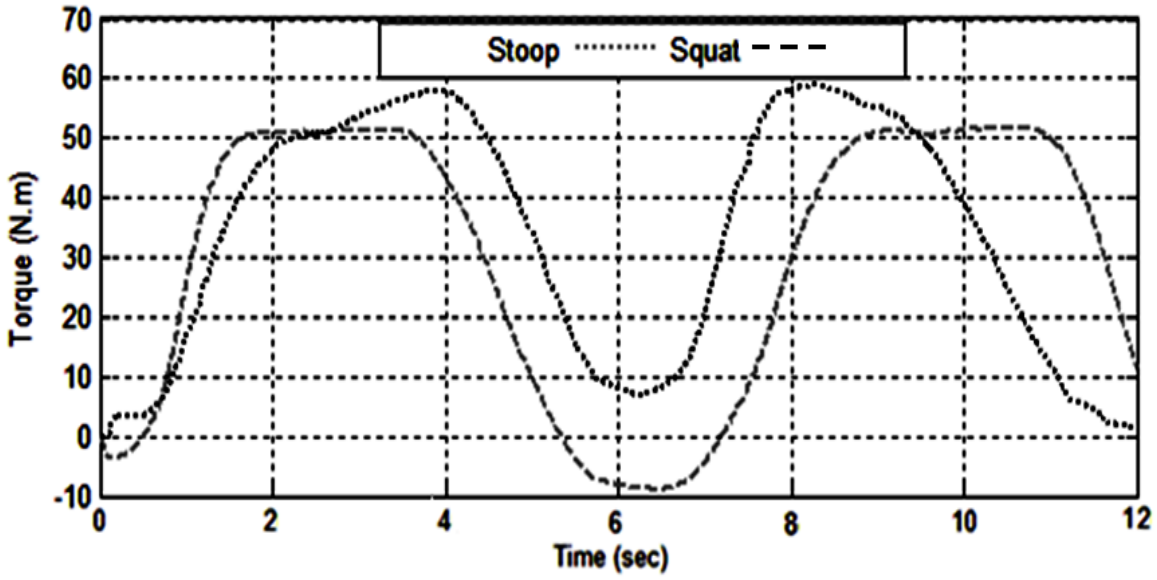

Figure 29 Comparison of Torque Requirement Between Lifting in Stoop Posture and Squat Posture

In Figure 29, while performing lift with the squat posture, HD is larger than it is in the stoop posture, which results in higher torque requirement during the lift with the squat posture.

This comparison has been made to show the behavior of the system in different cases. RMSE was performed for torque error between stoop and squat lifting posture and is shown in Figure 30. The error between the toque errors of the stoop and squat lift defines the different requirements of the torque assistance. The RMSE of torque error indicates that the control system performance is very consistent in both cases. The control system can also provide the torque depending on the required percent assistance and to see the performance of the controller at different percent assists, four different percent assists including 25, 50, 75 and 100% of assistance have been processed with the control system.

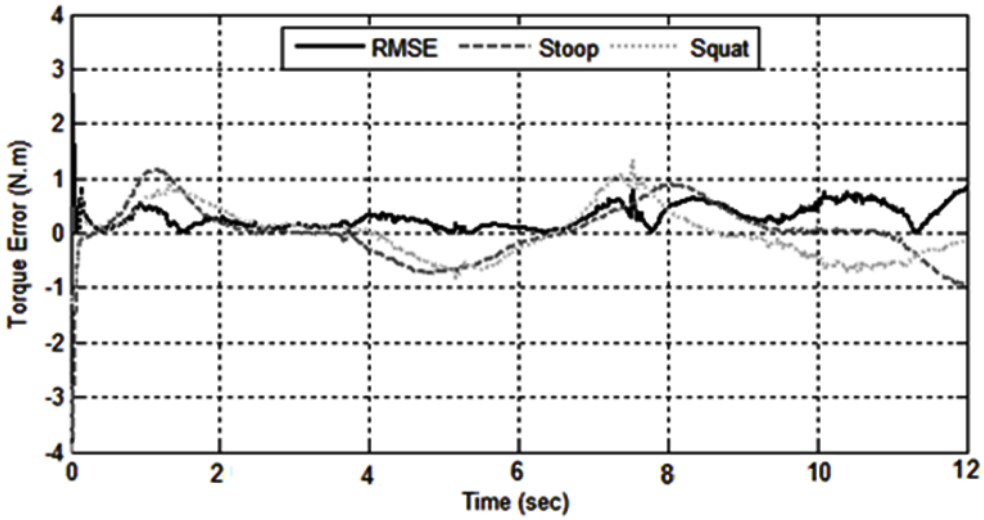

Figure 30 RMSE of Torque Error for Stoop Posture and Squat Posture Lift

In Figure 31, a generated torque pattern and difference by different percent assistance is shown. To find out the best system performance based on different percent assists, torque error (τ_desired–τ_obtained) comparisons are made and shown in Figure 32. All these results have been processed on the control system simulation with the same gain value. From the error plot, the highest error is detected from the 50% of assist followed by 25% of assist and then 75% of assist. The smallest error occurred with 100% of assist as compared to other cases. The reason behind getting more error in 50% assistance case cannot be defined by any specific parameter and remains unclear. The error at each assist value can be reduced by adjusting the PID gain values of the controller in the control system and may be valuable to investigate in future work. With 100% of assistance the error is very low because at this % assistance the torque requirement is more compatible with motor parameters and tuned PID gains of the control system.

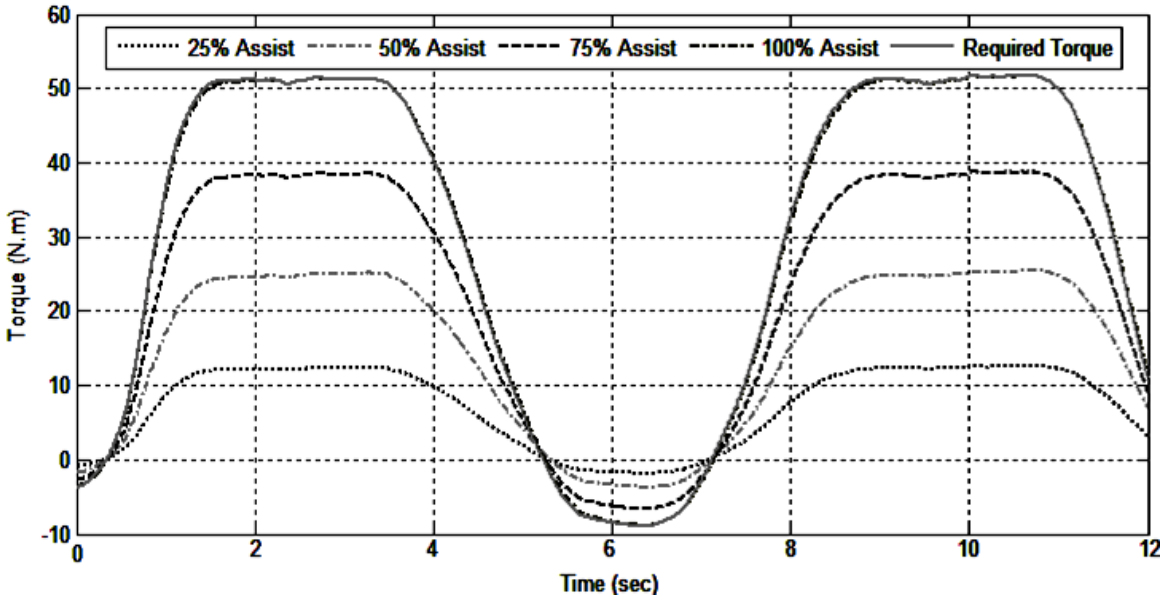

Figure 31 Comparison of Generated Torque from the Control System by % of Assistance

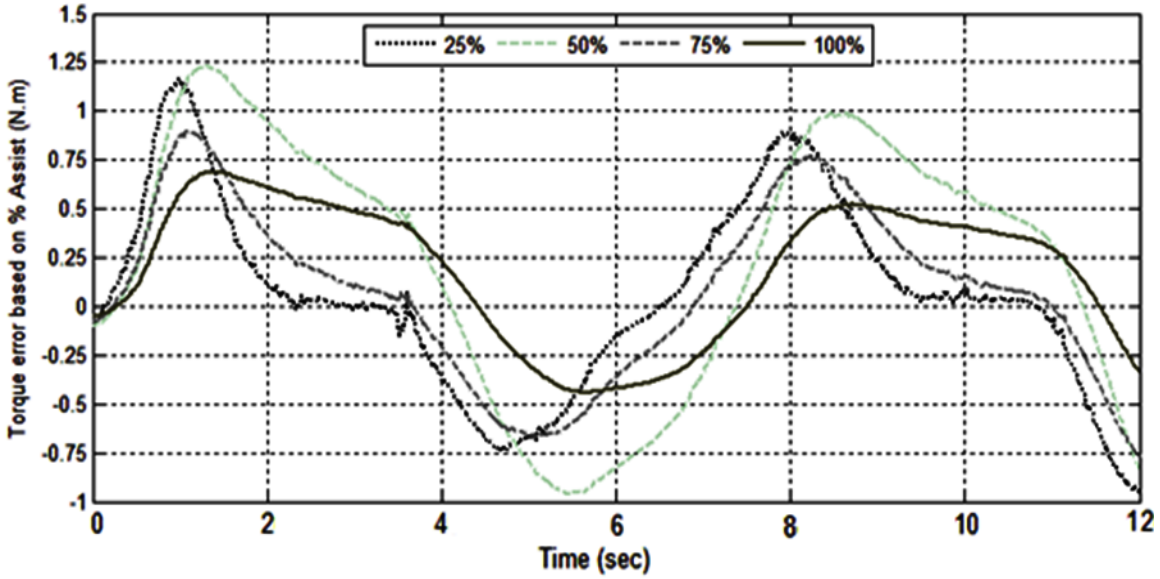

Figure 32 Comparison of Torque Error in the Control System by Different % Assists

There will be variances with the torque and speed outputs if the gain values are different. The current gain values are optimized according to the required torque and speed outputs from the control system, so that it can give the best tracking performance. Each gain has a different influence on the system performance including rise time, overshoot and steady state error. Using the current model conditions, optimized controller and existing motor parameters that were selected off the shelf from Midwest motions for this simulation, the control system appears to be working with great robustness and consistent performance.

4.3 Limitations

There are a few limitations of the system model and control system that should be mentioned.

From the current work in development of control system for LAD, force and COP parameters could be derived using more precise force measuring device to make the system more precise. With that one of the FFS has not contributed in the reaction force generation because of its position on the shoe sole. FFS would detect more force with asymmetrical lifting. In this study, however the body movements are considered only in an anterior/posterior direction, so it is not possible to discuss the control system performance while lifting in an asymmetry. The drawback with the selected motor is the weight of the motor and external gear head which is around 4.5 kg. The factor (weight of the motor and gear weight) might be a challenge to build the physical device.

5. CONCLUSION AND FUTURE SCOPE

This chapter presents conclusions based on the results and limitation of the studied work. From the results and recent work, a future scope is presented for this study.

5.1 Conclusion

The goal has been achieved by developing a control system with specific performance to provide assistance during lifting. Using an estimate of force and COP to predict HD and HD to predict the location of the load in hand, accurate required torque was derived. A statistically significant relationship was established between the reaction force from FFS and each FFS' locations on a shoe sole to calculate COP. A new function has been derived to predict HD with the R^2 value of 0.9069 and the function gives very close values compared to the direct experimental values from motion capture. This is one of the primary input sources behind a robustly working of the control system. In support of that, the statistical analysis result also shows high correlation between predicted HD and the HD data measured from motion capture. By using these inputs, the torque and speed output parameters from the control system were very consistent in the performance with different lifting postures and based on different percent assistance. Using an optimized PID controller to achieve reliable tracking performance and using motor model to attain the amount of torque generation, the system demonstrates acceptable performance for the hybrid lift assist device control system.

- Putting all together, a robust and accurate real-time control system has been developed with acceptable output results. Using this system as a baseline, a better working device can be modeled to serve the purpose of load lifting and material handling for the users.

5.2 Future Scope

- The future study can be done by incorporating the movements in the medial/lateral direction to explore the working boundaries of the control system and device.
- In the betterment of a future device, advanced and more accurate feedback devices can be used for much better results likewise replacing FFS by load cell and miniature force buttons for measuring the force and encoders for measuring the angles.
- Develop a physical prototype to test the control system.

APPENDIX

Pseudo Code

The command description read = input; display = output.

1. read torso angle (% all angles are converted from degree to radian)
2. read Center of Pressure (COP) value and force value
   2.1. conversion equation using COP and force to predict HD (horizontal distance from L5/S1 to Load in hand)
3. torque1 calculation using torso angle and L5/S1 to Load distance
   3.1. torque1 (Nm) = 0.5 x 9.81 x [(UBW x CTM)+(Load x L5/S1)] x sin(torso angle)
   (% this is a dynamic model equation to get the expected torque value)
   3.1.1. UBW = 0.48 x BW
   3.1.2. CTM = 0.23 x HT
4. read hip angle (% all angles are converted from degree to radian)
5. torque2 calculation using hip angle and pre-load value
   5.1. spring torque = (spring constant) x (hip angle)
   5.2. torque2 = (spring torque) + (pre-load value)
6. final torque = (torque1) – (torque2)
7. calculation for required percentage assistance
   7.1. torque to be controlled = (percentage of assistance) x (final torque)
8. Proportional Integral Derivative PID controller

8.1. current (I) = error x [Kp+(KdxS)+(Ki/s)]

8.1.1. error = (torque to be controlled - controlled torque)

9. motor torque

9.1. torque = (Ia x R – V – Kphi x w) x Kt/Ls

10. motor speed

10.1. speed= (Kphi x I – b) / Js

11. display torque = (motor torque) x N (% N is a gear ratio)

12. display speed = (motor speed) / N (% N is a gear ratio)

Matlab Simulink Model

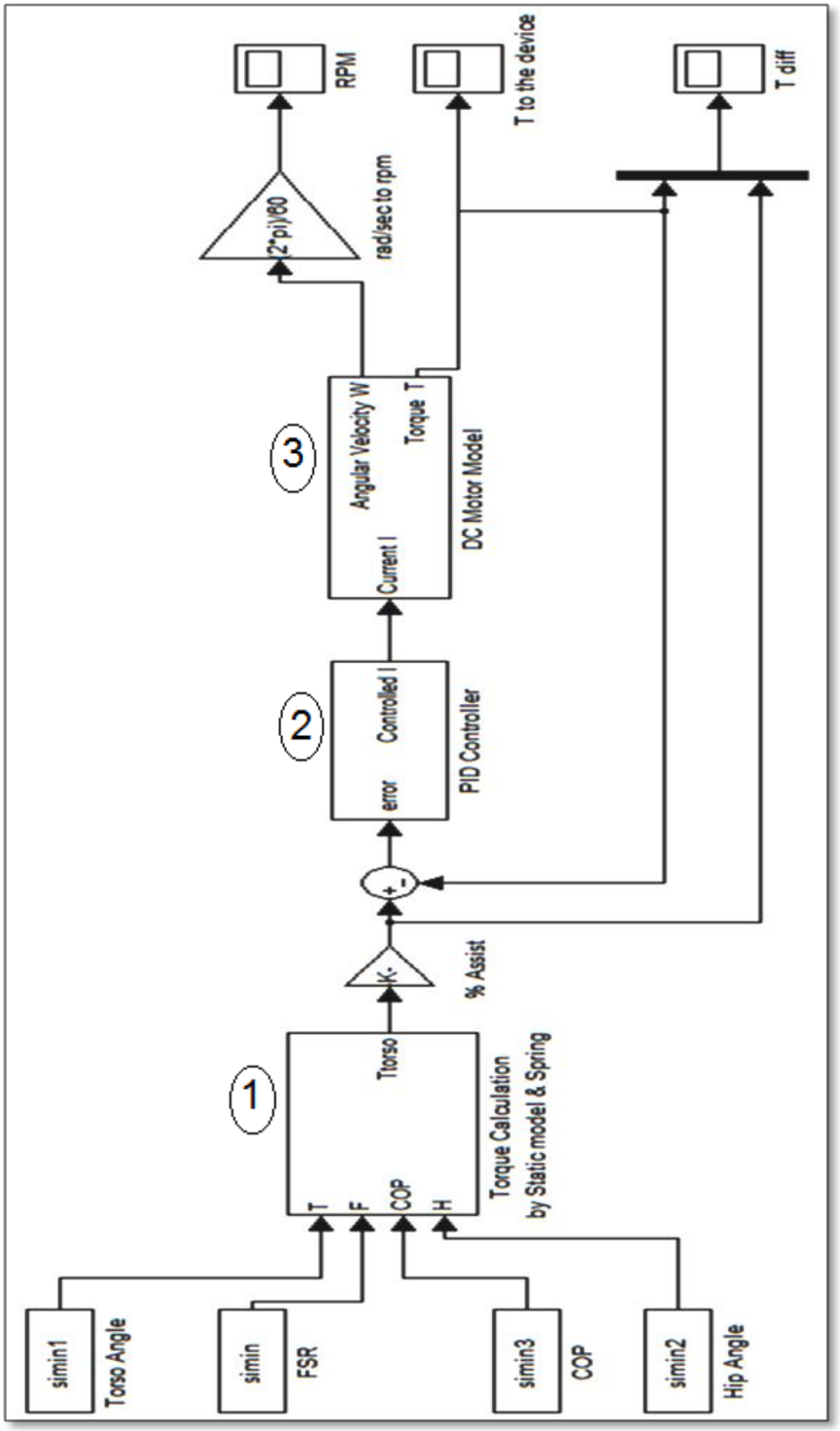

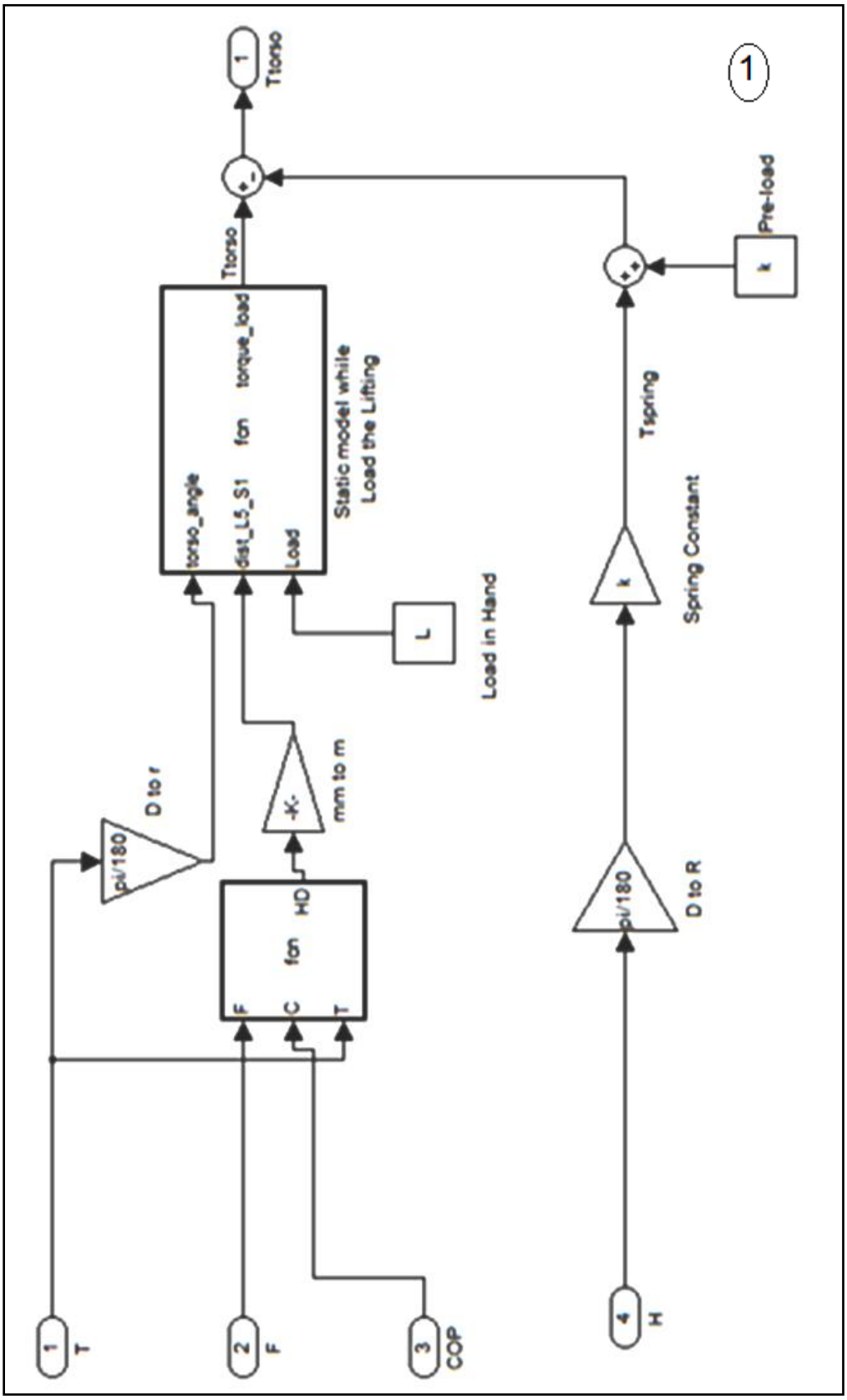
1
Ttorso
Tspring
Pre-load
Static model while
Load the Lifting
torso_angle
dist_L5_S1
fcn
torque_load
Load
Load in Hand
L
Spring Constant
D to r
pi/180
mm to m
D to R
HD
fcn
F
C
T
1
T
2
F
3
COP
4
H

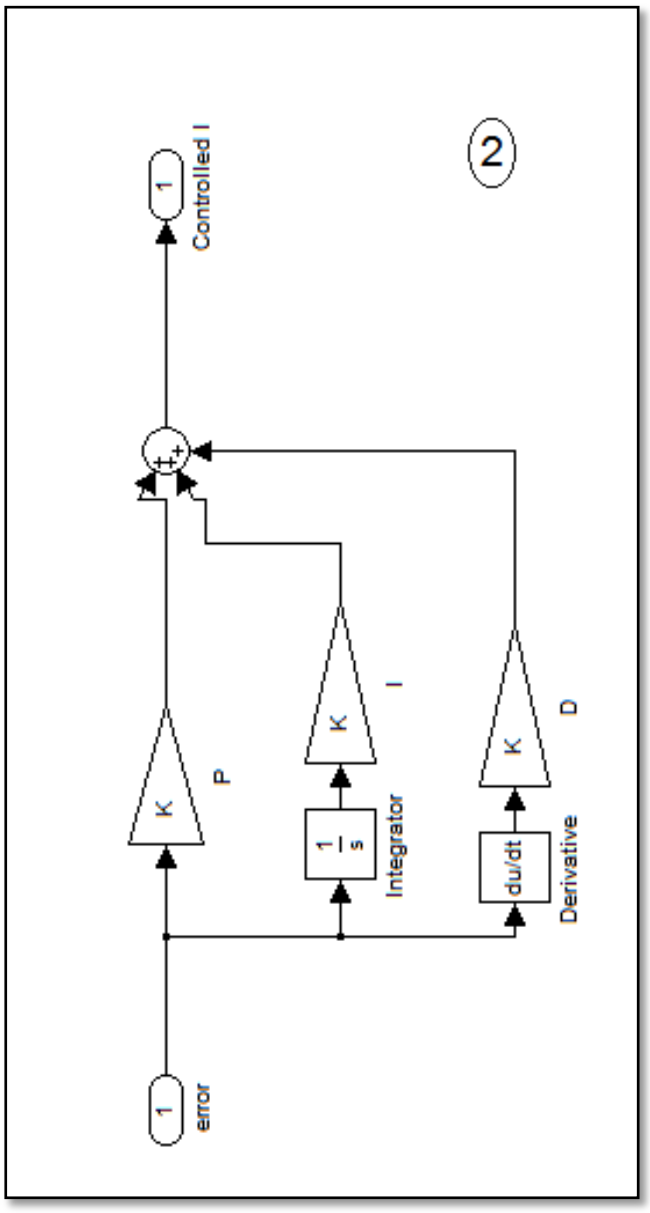
2
1
Controlled I
K
P
K
I
K
D
1
s
Integrator
du/dt
Derivative
1
error

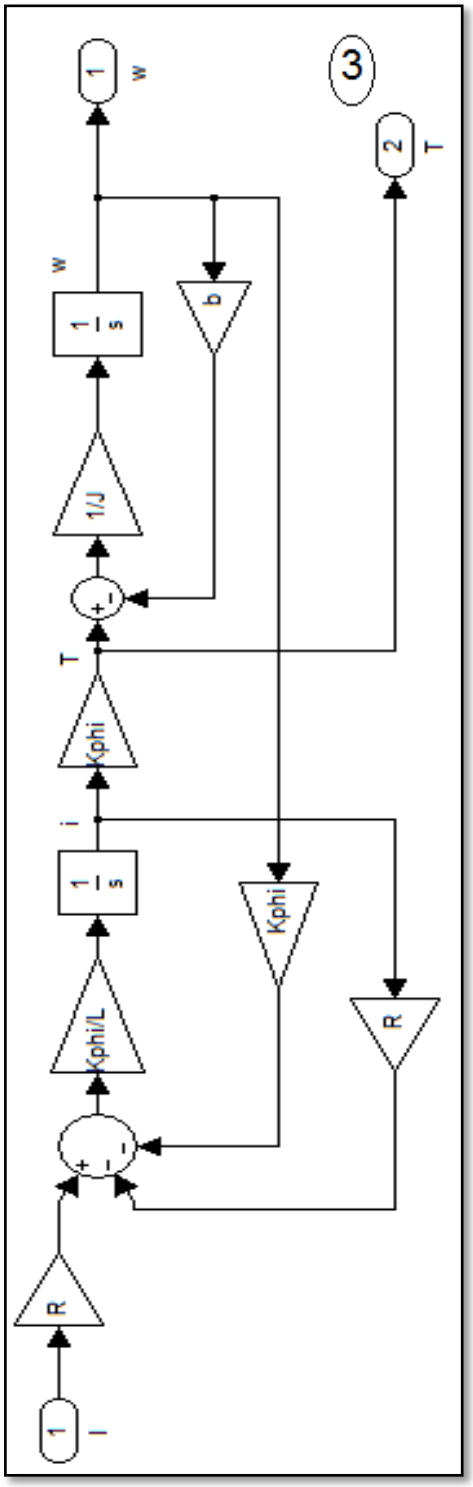
1
w
3
2
T
w
b
1
s
1/J
T
Kphi
i
1
s
Kphi
Kphi/L
R
R
1
I

REFERENCES

[1] C. Lotz A., Michael J. Agnew, A. Godwin A., and J. Stevenso M., "The effect of an on-body personal lift assist device (PLAD) on fatigue during a repetitive lifting task," *Journal of Electromyography and Kinesiology*, vol. 19, no. 2009, pp. 331-340, 2007.

[2] C. De Luca, "Low back pain: a major problem with low priority," *Journal of Rhabilitation Research & Development*, vol. 4, no. vii, p. 34, 1997.

[3] S. Lavender, K. Shakeel, G. Andersson, and J. Thomas, "Effects of a lifting belt on spine moments and muscle recruitments after unexpected sudden loading," *Spine*, vol. 25, no. 12, pp. 1569-1579, 2000.

[4] Brammer, Christopher D., University of Utah, "Using biomechanical analysis and user feedback to evaluate optimal design specifications in lift assist devices," 2011-12.

[5] E. M. Sadler, R. B. Graham, and J. M. Stevenson, "The personal lift-assist device and lifting technique: a principal component analysis," *Ergonomics*, vol. 54, pp. 392-402, 2011.

[6] R. B. Graham, E. M. Sadler, and J. M. Stevenson, "Does the personal lift-assist device affect the local dynamic stability of the spine during lifting?," *Journal of Biomechanics*, vol. 44, pp. 461-466, 2011.

[7] D. Nielsen and J. Austin, "Preventing back injuries in hospital settings: the effects of video modeling on safe patient lifting by nurses," *Journal of Applied Behavior Analysis*, vol. 42, no. 3, pp. 551-561, 2008.

[8] "Musculoskeletal Disorders and Workplace Factors Chapter 6. Low-Back Musculoskeletal Disorders: Evidence for Work-Relatedness," NIOSH Publication, pp. 97-141, 1997.

[9] Jonathan Cluett, M.D., "Low Back Pain and Lumber Back Pain," [Online]. Available: http://www.about.com, May 2010.

[10] "Nonfatal cases involving days away from work: Selected characteristics," *Bureau of Labor Statistics Data*, 2003.

[11] "Low Back Pain in worker," MFL Occupational Health Centre Inc., 2003.

[12] "Back Pain at work: Preventing pain and injury," Mayo Foundation for Medical Education and Research.

[13] Judith Groch, Reviewed by Zalman S. Agus, MD, Emeritus Professor University of Pennsylvania School of Medicine "Herniated Disc Back Surgery-Back Surgery Cost," Published: September 11, 2008.

[14] O. Carol, M. McFarland,"Rehabilitation and Exercise Following Spine Surgery."

[15] D. Gagnon and M. Gagnon, "The influence of dynamic factors on tri-axial net muscular moments at the L5/S1 joint during asymmetrical lifting and lowering.," *Journal of Biomechanics*, vol. 25, pp. 891-901, 1992.

[16] D. Bloswick, K. Greenland, A. Merryweather, "Prediction of peak back compressive forces as a function of lifting speed and compressive forces at lift origin and destination - a pilot study.," *Safety Health Work*, vol. 2, pp. 236-242, 2011.

[17] A. Merryweather, D. Bloswick, and R. Sesek, "A calculation of dynamic back compressive force: a pilot study of identify load displacement velocity constants.," *Journal of SH&E Research*, vol. 5, pp. 1-15, 2008.

[18] "Springzback," Babcock Innovation Inc., [Online]. Available: http://www.springzback.com, 2011.

[19] Kazerooni, H, R. Steger, L. Huang "Hybrid control of the Berkeley Lower Extremity Exoskeleton, *The International Journal of Robotics Research*, V25, No 5-6, pp. 561-573, May-June 2006.

[20] A. Merryweather, M. Loertscher, and D. Bloswick, "A revised back compressive force estimation model for ergonomic evaluation of lifting tasks.," *Journal of Prevention, Assessment and Rehabilitation*, vol. 34, no. 3, pp. 263-272, 2009.

[21] Araki M., Kyoto University, Japan, "PID Control," Control Systems, Robotics and Automation -Vol. II.

[22] Professor Bill Messner, Carnegie Mellon University and Professor Dawn Tilbury, University of Michigan, "Controls tutorial of Matlab for PID controller," [Online]. Available: http://www.engin.umich.edu/group/ctm/PID/PID.html.

[23] "Vicon Nexus system and camera systems for motion capture." [Online]. Available: http://www.vicon.com/products.

[24] "Placement Protocols for Plugin-Gait marker Placement," Vicon Documentation & Notes, Preparation v1.2.

[25] "FlexiForce Sensor User Manual (Rev G)," *Flexiforce- Standard force and load sensor*, [Online].
Available: http://www.tekscan.com/flexible-force-sensors#specifications.

[26] "Flexi Force Sensor Structure", [Online].
Available: http://www.tekscan.com/flexible-force-sensors#specifications.

[27] M. Eindhoven and P. Dekker, "Zero-moment point method for stable biped walking," 2009.

[28] D. A. Winter, "Human balance and posture control during standing and walking," Gait and Posture, vol. 3, no. 4, pp. 193–214, Dec. 1995.

[29] D. C. Ferencz, Z. Jin, and H. J. Chizeck, "Estimation of center-of-pressure during gait using an instrumented ankle-foot orthosis," in *Engineering in Medicine and Biology Society*, 1993, pp. 981-982.